



entropy



Article

Time-Dependent Effective Hamiltonians for Light–Matter Interactions

Aroaldo S. Santos, Pedro H. Pereira, Patrícia P. Abrantes, Carlos Farina, Paulo A. Maia Neto and Reinaldo de Melo e Souza

Special Issue

Dynamics of Open Quantum Systems: Quantum Fluctuations, Decoherence and Emergent Phenomena

Edited by



Dr. Fernando C. Lombardo and Dr. Paula I. Villar



<https://doi.org/10.3390/e26060527>

Article

Time-Dependent Effective Hamiltonians for Light–Matter Interactions

Aroaldo S. Santos ^{1,2}, Pedro H. Pereira ¹, Patrícia P. Abrantes ³ , Carlos Farina ³, Paulo A. Maia Neto ^{3,*} 
and Reinaldo de Melo e Souza ¹ 

¹ Instituto de Física, Universidade Federal Fluminense, Niterói 24210-346, Rio de Janeiro, Brazil; arofisica@gmail.com (A.S.S.); pedro_h@id.uff.br (P.H.P.); reinaldos@id.uff.br (R.d.M.e.S.)

² Instituto Federal do Paraná, Telêmaco Borba 84269-090, Paraná, Brazil

³ Instituto de Física, Universidade Federal do Rio de Janeiro, Rio de Janeiro 21941-972, Rio de Janeiro, Brazil; ppabrantes91@gmail.com (P.P.A.); farina@if.ufrj.br (C.F.)

* Correspondence: pamn@if.ufrj.br

Abstract: In this paper, we present a systematic approach to building useful time-dependent effective Hamiltonians in molecular quantum electrodynamics. The method is based on considering part of the system as an open quantum system and choosing a convenient unitary transformation based on the evolution operator. We illustrate our formalism by obtaining four Hamiltonians, each suitable to a different class of applications. We show that we may treat several effects of molecular quantum electrodynamics with a direct first-order perturbation theory. In addition, our effective Hamiltonians shed light on interesting physical aspects that are not explicit when employing more standard approaches. As applications, we discuss three examples: two-photon spontaneous emission, resonance energy transfer, and dispersion interactions.

Keywords: effective Hamiltonians; time-dependent Hamiltonians; quantum fluctuations; molecular quantum electrodynamics; light–matter interactions



Citation: Santos, A.S.; Pereira, P.H.; Abrantes, P.P.; Farina, C.; Maia Neto, P.A.; de Melo e Souza, R. Time-Dependent Effective Hamiltonians for Light–Matter Interactions. *Entropy* **2024**, *26*, 527. <https://doi.org/10.3390/e26060527>

Academic Editors: Fernando C. Lombardo and Paula I. Villar

Received: 27 May 2024

Revised: 12 June 2024

Accepted: 14 June 2024

Published: 19 June 2024



Copyright: © 2024 by the authors. Licensee MDPI, Basel, Switzerland. This article is an open access article distributed under the terms and conditions of the Creative Commons Attribution (CC BY) license (<https://creativecommons.org/licenses/by/4.0/>).

1. Introduction

In molecular quantum electrodynamics, atoms and molecules are treated within non-relativistic quantum mechanics, and the electromagnetic field mediating the interactions is quantized. This approach, born with Dirac’s seminal treatment of spontaneous emission [1], is still an ongoing and intense research field, especially with the unprecedented control of light–matter interactions at the atomic scale reached in the last decades.

All phenomena in this topic can be fully understood by starting with the classical minimal coupling Hamiltonian and quantizing it. For molecular quantum electrodynamics, the most convenient approach is to work in the Coulomb gauge. Throughout this work, we shall deal with neutral molecules, in which case we can make a unitary transformation on the minimal coupling Hamiltonian and work with the equivalent multipolar Hamiltonian [2–6]. Nonetheless, the generality of these Hamiltonians is also their main weakness, since we must perform extensive calculations to obtain the quantities describing most of the effects. For instance, the interaction between two nonpolar molecules in their ground state results from a tedious fourth-order perturbative calculation.

Here comes the convenience of working with effective Hamiltonians, which are tailored for each specific application, bringing several physical insights and shortening the technical calculation to a much simpler and lower perturbative order analysis. An insightful example is the dynamical polarizability (DP) Hamiltonian, obtained by R. Passante and collaborators [7,8], which is built directly on the molecular dynamical polarizability instead of its electric dipole operator, capturing better the physics governing the interaction. Indeed, nonpolar molecules do not possess permanent electric dipole moments, and their interaction is possible only due to virtual internal transitions that are automatically taken into

account by the dynamical polarizability. This is the main message of effective Hamiltonians: building the relevant physical mechanism into the Hamiltonian lowers the perturbative order required in calculations. With the DP Hamiltonian, intermolecular interactions are determined by means of a second-order calculation. Effective Hamiltonians and actions are also useful in describing non-stationary systems and have been employed to develop a multipolar approach to the dynamical Casimir effect [9] and to understand its microscopic origin [10–14].

Effective Hamiltonians are easily constructed from unitary transformations [15], but there is no general recipe to generate useful ones. In this paper, we fill this gap by presenting a systematic method to obtain convenient effective Hamiltonians and by discussing their physical implications. To illustrate our approach, we derive four general effective Hamiltonians allowing us to extend the scope of applications to important phenomena in molecular quantum electrodynamics.

Our method is based on choosing a unitary transformation inspired by (but not equal to) the Hermitian conjugate of the evolution operator for the system. A key concept for our formalism is that the linear susceptibility χ of a quantum system is built from the unequal time commutator of an appropriate operator \mathcal{O} describing the system. For the context explored in this paper, we shall take \mathcal{O} as being (i) the molecular dipole operator, in which case χ is related to the molecular polarizability, and (ii) the electric field operator, with χ representing the electric field generated by a point dipole (Green function), as discussed in Appendix A.

The importance of the unequal time commutators of the electric field operators in connection to the measurability of the fields was stressed in the literature [16,17]. Here, we show that the unequal time commutators can be taken as the basis to generate convenient effective Hamiltonians by allowing a given degree of freedom to effectively dress another one. Physically, this is equivalent to considering part of our system (a molecule or the electromagnetic field) as an open quantum system that is effectively dressed by an appropriate unitary evolution operator, thus yielding an effective time-dependent Hamiltonian for the system.

In Section 2, we employ our formalism to set up the Hamiltonian H_M^{eff} , in which the molecular degrees of freedom are dressed by the field. This Hamiltonian generalizes the DP one in two aspects: (i) it naturally accounts for internal dissipation in the molecules, and (ii) it does not require the molecules to remain in the same internal state (usually the ground state) during the process to be described. The latter aspect is a key element and enables us to evaluate the two-photon spontaneous emission (TPSE) in Section 3 within first-order perturbation theory—a much simpler route than the one commonly followed in the literature.

From Section 4 on, we work with situations involving more than one molecule. We employ our method to build the second effective Hamiltonian H_F^{eff} , where one molecule, say molecule B , dresses the field. With this dressing, the field acting on the other molecules is given by the superposition of the vacuum electric field with the electric dipole field generated by B . In Section 5, we demonstrate the convenience of H_F^{eff} by directly computing the resonance energy transfer (RET) between two quantum emitters in first order.

Then, in Section 6, we analyze dipole–dipole correlation effects and show that different effective Hamiltonians are convenient depending on the distance separating the molecules. In the asymptotic long-distance limit, we demonstrate the Hamiltonian H_{MF}^{eff} , in which the field dresses the molecules, and, in turn, one of the dressed molecules dresses back the field. This Hamiltonian is similar to H_F^{eff} , but now the electric field generated by molecule B does not depend on the molecular dipole operator. Instead, it is produced by the dipole induced by the vacuum itself. In the particular case where we assume the molecules to be in the ground state, in the long-distance limit, we recover the Hamiltonian originally proposed by P.W. Milonni [18].

Finally, for the short-distance limit (the non-retarded regime), we follow a complementary route: first, one molecule dresses the field, and then the dressed field dresses

back the molecules. This leads us to a new effective Hamiltonian $H_{\text{FM}}^{\text{eff}}$. We demonstrate its convenience by applying it in Section 7 to obtain the London interaction energy in first-order perturbation theory and show that this route provides some relevant physical insights. Indeed, our approach can quantify the contributions to the interaction energy coming from the dipole fluctuations of each molecule. The above examples surely do not exhaust the list of useful effective Hamiltonians, and our method should be valuable for several additional applications.

2. The Field Dresses the Molecules

We begin with a single neutral molecule at position \mathbf{R} in the presence of the quantized electromagnetic field. In the dipole approximation, the Hamiltonian describing the system is

$$H_{\text{total}} = H_0 - \mathbf{d} \cdot \mathbf{E}(\mathbf{R}), \quad (1)$$

where \mathbf{d} is the molecular dipole operator, and $\mathbf{E}(\mathbf{R})$ is the quantized electric field evaluated at the molecule's center-of-mass position \mathbf{R} . Note that in the dipole approximation, the electric field can be taken as uniform over the scale of the molecule. H_0 stands for the free Hamiltonians and is given by

$$H_0 = H_{0m} + \sum_{\mathbf{k}\sigma} \hbar\omega_{\mathbf{k}} \left(a_{\mathbf{k}\sigma}^\dagger a_{\mathbf{k}\sigma} + \frac{1}{2} \right). \quad (2)$$

In this expression $a_{\mathbf{k}\sigma}$ ($a_{\mathbf{k}\sigma}^\dagger$) stands for the annihilation (creation) operator for a photon with wavevector \mathbf{k} and polarization σ , whose electromagnetic field oscillates with a frequency $\omega_{\mathbf{k}} = |\mathbf{k}|c$. H_{0m} is the free molecular Hamiltonian whose eigenstates and eigenenergies are assumed to be known. The coupling between the molecule and field, given by the second term on the right-hand side of Equation (1), can be treated as a perturbation. Therefore, it is convenient to work in the interaction picture with the interaction Hamiltonian

$$H(t) = -\mathbf{d}(t) \cdot \mathbf{E}(\mathbf{R}, t). \quad (3)$$

The time dependence is obtained by evolving the operators with the free Hamiltonian H_0 . A nonpolar molecule is characterized by not having a permanent electric dipole in its ground state $|g\rangle$, i.e., $\langle g|\mathbf{d}|g\rangle = \mathbf{0}$. Thus, any process during which the molecule does not excite, such as the Stark shift, must be obtained at least through second-order perturbation theory. If $|\psi(t)\rangle$ symbolizes the state of the molecule-field system in the interaction picture, then its evolution can be written as

$$i\hbar \frac{d}{dt} |\psi(t)\rangle = H(t) |\psi(t)\rangle. \quad (4)$$

An equivalent description is generated once we apply a unitary transformation to the state. We choose it as

$$U_{\text{M}}(t) = e^{\frac{i}{\hbar} \int_{-\infty}^t dt' H(t')}. \quad (5)$$

Note that transformation (5) implements the Heisenberg picture to first order in H , thus canceling, at this order, the time evolution of $|\psi(t)\rangle$, which is precisely our goal. If $[H(t), H(t')] = 0$, then the transformation given in Equation (5) would implement the Heisenberg picture exactly. Therefore, in the representation defined by U_{M} , the time evolution of $|\psi(t)\rangle$ results from the non-vanishing value of the commutator $[H(t), H(t')]$, which is consistent with the discussion on linear susceptibilities outlined in Section 1. As will become clear below, this transformation effectively dresses the molecular degree of freedom indicated by the subscript M. Next, we derive the equation satisfied by $|\psi_{\text{M}}(t)\rangle = U_{\text{M}}|\psi(t)\rangle$. From Equation (4), we find

$$i\hbar \frac{d}{dt} |\psi_{\text{M}}(t)\rangle = H_{\text{M}} |\psi_{\text{M}}(t)\rangle, \quad (6)$$

with

$$H_M(t) = U_M(t)H(t)U_M(t)^{-1} + i\hbar \frac{dU_M(t)}{dt} U_M^{-1}(t). \quad (7)$$

Here enters the fact that we are not looking for an equivalent Hamiltonian but rather an effective one. We desire an equivalent Hamiltonian only up to quadratic order in the dipole operator, and thus, we are allowed to expand U_M and collect results up to the second order in H , obtaining

$$U_M(t) \approx 1 + \frac{i}{\hbar} \int_{-\infty}^t dt' H(t') - \frac{1}{2\hbar^2} \left[\int_{-\infty}^t dt' H(t') \right]^2, \quad (8)$$

$$\frac{d}{dt} U_M(t) \approx \frac{i}{\hbar} H(t) - \frac{1}{2\hbar^2} \int_{-\infty}^t dt' \{H(t), H(t')\}. \quad (9)$$

Note that the expansion in Equation (8) does not correspond to a Dyson series, since the unitary transformation given in Equation (5) is not an evolution operator (it lacks a time-ordering operator). These expansions differ in the second-order term, and we stress that the third term on the right side of Equation (8) is proportional to the square of the second term, which is crucial for the results we will obtain. We define the effective Hamiltonian $H_M^{\text{eff}}(t)$ as the second-order approximation of H_M , which is obtained by substituting the previous relations into Equation (7):

$$H_M^{\text{eff}}(t) = -\frac{i}{2\hbar} \int_{-\infty}^t dt' [H(t), H(t')], \quad (10)$$

where we used the identity $2H(t)H(t') = [H(t), H(t')] + \{H(t), H(t')\}$. Notice that the linear term in the dipole vanished. From Equation (3) and since electric field operators at the same spatial point commute at all times (see Appendix A), we are left with

$$H_M^{\text{eff}}(t) = -\frac{i}{2\hbar} \int_{-\infty}^t dt' [d_j(t), d_l(t')] E_j(\mathbf{R}, t) E_l(\mathbf{R}, t'), \quad (11)$$

where we employed Einstein notation and denoted by $j, l = 1, 2, 3$ the Cartesian components of the operators. The great convenience of this Hamiltonian is that it is quadratic in the operators, thus halving the required perturbation order in comparison to the Hamiltonian given by Equation (3). We point out that our demonstration remains the same whether the electric field is quantized or not. As an example, with this effective Hamiltonian, the Stark effect can be obtained from a first-order perturbative calculation. We emphasize that this Hamiltonian is valid only within first-order perturbation theory, but improvements can be made if one keeps extra terms in Equations (8) and (9). H_M^{eff} mixes both the materials' and fields' degrees of freedom. When the atom is assumed to remain in the ground state, we may take the expectation value of H_M^{eff} in the molecular's subspace defined by the ground state through the evaluation of $\langle g | H_M^{\text{eff}}(t) | g \rangle$. We stress here that we are not acting on the field subspace, and thus, this average is still an operator in the field variables, which we denote by

$$H_M^{\text{eff}(gg)}(t) = -\frac{1}{2} \int_{-\infty}^{\infty} dt' \alpha_{jl}(t - t') E_j(\mathbf{R}, t) E_l(\mathbf{R}, t'), \quad (12)$$

with

$$\alpha_{jl}(t - t') = \frac{i}{\hbar} \theta(t - t') \langle g | [d_j(t), d_l(t')] | g \rangle \quad (13)$$

being the molecular dynamical polarizability tensor for the ground state describing its linear response to an applied electric field—see Appendix A for details. For practical applications and some physical interpretations, it is generally more suitable to work with

the dynamical polarizability in the Fourier representation rather than in the time domain. To do so, we write the free electromagnetic field in the usual form:

$$E(\mathbf{R}, t') = \sum_{k\sigma} E_{k\sigma}(\mathbf{R}, t') = \sum_{k\sigma} \left[E_{k\sigma}^{(+)}(\mathbf{R}) e^{-i\omega_k t'} + E_{k\sigma}^{(-)}(\mathbf{R}) e^{i\omega_k t'} \right], \quad (14)$$

where $\omega_k = c|k|$, σ is the polarization degree of freedom, and the superscript $+$ ($-$) refers to positive (negative) frequencies of the field. Substituting Equation (14) into (12), we arrive at

$$H_M^{\text{eff}(gg)}(t) = -\frac{1}{2} \mathbf{d}^{\text{ind}}(t) \cdot E(\mathbf{R}, t), \quad (15)$$

where

$$\mathbf{d}_j^{\text{ind}}(t) = \sum_{k\sigma} \left[\alpha_{jl}(\omega_k) E_{k\sigma}^{l(+)}(\mathbf{R}, t) + \alpha_{jl}(-\omega_k) E_{k\sigma}^{l(-)}(\mathbf{R}, t) \right] \quad (16)$$

stands for the vacuum-induced dipole operator, and $E_{k\sigma}^{l(\pm)}(\mathbf{R}, t) = E_{k\sigma}^{l(\pm)}(\mathbf{R}) e^{\mp i\omega_k t}$ is the l -th Cartesian component of $E_{k\sigma}^{(\pm)}(\mathbf{R}, t)$. Notice that $\mathbf{d}^{\text{ind}}(t)$ acts on the field's Hilbert space. Due to the reality of $\alpha(t - t')$, $\alpha_{jl}(-\omega_k) = \alpha_{jl}^*(\omega_k)$, and, thus, $\mathbf{d}^{\text{ind}}(t)$ is an Hermitian operator. If dissipation is negligible, we re-obtain as a particular case the DP Hamiltonian [7]

$$H_M^{\text{eff}(DP)}(t) = -\frac{1}{2} \sum_{k\sigma} \alpha_{jl}(\omega_k) E_{k\sigma}^l(\mathbf{R}, t) E^j(\mathbf{R}, t). \quad (17)$$

Physically, this is the quantum counterpart of the interaction energy of a polarizable system without permanent electric dipole moments in the presence of an external electric field. In the case without dissipation, the dynamical polarizability in the Fourier space is given by (see Appendix A)

$$\alpha_{jl}(\omega) = -\frac{1}{\hbar} \sum_{r \neq g} d_j^{gr} d_l^{rg} \left(\frac{1}{\omega - \omega_{rg}} - \frac{1}{\omega + \omega_{rg}} \right), \quad (18)$$

where r denotes the excited internal molecular states, and $\mathbf{d}^{gr} = \langle g | \mathbf{d} | r \rangle = \mathbf{d}^{rg*}$ is the transition dipole moment between states g and r , while ω_{rg} is the corresponding transition frequency.

There are some subtleties concerning the unitary transformation employed in this section. One could argue that once the integration present in Equation (5) starts from $-\infty$, our truncation in Equation (9) is not rigorous. The point is that the molecule has a finite memory, characterized by a time scale τ . This means that $\alpha_{jl}(t - t')$ vanishes for $t - t' \gg \tau$ in Equation (13), enabling the lower limit in (5) to be replaced by $t - \tau$. The validity of this truncation is then tantamount to the validity of the perturbative method in the molecule-field interaction, justifying our approach. This argument also underlies the convenience of working in the Fourier space. Convergence of the time integration in Equation (12) requires that we account for dissipation in the polarizability. Nevertheless, in many cases of interest, the most relevant Fourier modes are far from molecular resonances, and we may neglect dissipation when using Equations (15) and (16).

Another important aspect is that the effective Hamiltonian (11) is convenient only when first-order perturbation theory in Hamiltonian (3) vanishes, even though regularization techniques may render it applicable if this is not the case [8]. We may separate the main applications of the effective Hamiltonian H_M^{eff} into two groups: (i) the molecule remains in the same internal state during the entire process, and the expectation value of the electric dipole operator in this state is zero; (ii) the molecule undergoes a transition between two internal states, but the electric dipole operator is unable to connect these two states. Examples involving (i) have already been discussed in the literature [7,8], in contrast with case (ii). One fascinating example of this second group is the two-photon spontaneous emission, with selection rules forbidding the one-photon transition. In the next section,

we explore this example from the perspective of the effective Hamiltonian derived in this section.

3. Application to the Two-Photon Spontaneous Emission

An excited molecule may decay to its ground state through the emission of two photons in the so-called two-photon spontaneous emission (TPSE). This phenomenon is particularly interesting when the one-photon transition is forbidden. The TPSE makes the vacuum unstable and is responsible for the initial buildup of the intracavity field in two-photon micromasers [19–21]. More recently, it was shown that the simultaneously emitted photons can be indistinguishable and entangled in time and frequency [22–24], renewing the interest in this phenomenon [25–29]. This section aims to obtain the TPSE rate directly from first-order perturbation theory in Hamiltonian (11). Let us consider that a molecule in an internal state $|e\rangle$ decays in vacuum to its ground state $|g\rangle$ through the emission of two photons with wavevectors \mathbf{k} and \mathbf{k}' and polarizations σ and σ' . To this end, it suffices to analyze the matrix element of H_M^{eff} connecting the initial and the final states, given by

$$\langle g; 1_{\mathbf{k}\sigma} 1_{\mathbf{k}'\sigma'} | H_M^{\text{eff}}(t) | e; 0 \rangle = -\frac{1}{2} \int_{-\infty}^{\infty} dt' D_{jl}^{ge}(t, t') \langle 1_{\mathbf{k}\sigma} 1_{\mathbf{k}'\sigma'} | E_j(\mathbf{0}, t) E_l(\mathbf{0}, t') | 0 \rangle, \quad (19)$$

where we chose the origin of our coordinate system at the position of the molecule. Here, $|0\rangle$ denotes the vacuum state of the electromagnetic field. We also define

$$D_{jl}^{ge}(t, t') = \frac{i}{\hbar} \theta(t - t') \langle g | [d_j(t), d_l(t')] | e \rangle, \quad (20)$$

which involves only the molecular degrees of freedom and quantifies the linear response of the molecule to an applied field connecting internal states $|e\rangle$ and $|g\rangle$. Note that, when taking $|e\rangle = |g\rangle$ in Equation (20), the tensor \overleftrightarrow{D} yields as a particular case the polarizability of the molecule, which is given by Equation (13). The TPSE rate is immediately obtained in the long-time limit by substituting Equation (19) into Fermi's golden rule. In general, it is more convenient to represent \overleftrightarrow{D} in Fourier space. We begin by writing

$$\mathbf{d}(t) = e^{iH_{0m}(t-t_0)} \mathbf{d} e^{-iH_{0m}(t-t_0)} \quad (21)$$

and, at the end, we take $t_0 \rightarrow -\infty$. In this expression, H_{0m} denotes the free molecular Hamiltonian, with eigenstates satisfying $H_{0m}|r\rangle = \hbar\omega_r|r\rangle$, so that by inserting a closure relation $\mathbb{I} = \sum_r |r\rangle\langle r|$ into Equation (20), we obtain

$$D_{jl}^{ge}(t, t') = \alpha_{jl}^{ge}(t - t') e^{-i\omega_{eg}t'}, \quad (22)$$

with

$$\alpha_{jl}^{ge}(t - t') = \frac{i}{\hbar} \theta(t - t') \sum_r \left[d_j^{gr} d_l^{re} e^{-i\omega_{rg}(t-t')} - d_l^{gr} d_j^{re} e^{i\omega_{re}(t-t')} \right]. \quad (23)$$

The instant t_0 plays a role only in an unimportant global phase, which was discarded. In Fourier space, Equation (23) becomes

$$\alpha_{jl}^{ge}(\omega) = \frac{1}{\hbar} \sum_r \left(\frac{d_j^{gr} d_l^{re}}{\omega_{rg} - \omega} + \frac{d_l^{gr} d_j^{re}}{\omega_{re} + \omega} \right). \quad (24)$$

The desired matrix element given in Equation (19) can be obtained from Equation (14). For emission processes, only positive frequency modes contribute. Using Equation (22), we also obtain

$$\begin{aligned} \langle g; 1_{k\sigma} 1_{k'\sigma'} | H_M^{\text{eff}}(t) | e; 0 \rangle &= \frac{\hbar \sqrt{\omega_k \omega_{k'}}}{4\epsilon_0 V} e^{i(\omega_k + \omega_{k'} - \omega_{eg})t} \times \\ &\quad \left[\epsilon_{k\sigma}^j \epsilon_{k'\sigma'}^l \alpha_{jl}^{ge} (\omega_{eg} - \omega_{k'}) + \epsilon_{k'\sigma'}^j \epsilon_{k\sigma}^l \alpha_{jl}^{ge} (\omega_{eg} - \omega_k) \right], \end{aligned} \quad (25)$$

where $\epsilon_{k\sigma}^j$ is the j th Cartesian component of the polarization unit vector for the mode with wavevector k and polarization σ , and V is the volume of the quantization box. In the long-time limit, we are interested in photon pairs satisfying the condition $\omega_k + \omega_{k'} = \omega_{eg}$. With this, we see that $\alpha_{jl}(\omega_{eg} - \omega_{k'}) = \alpha_{jl}(\omega_k) = \alpha_{lj}(\omega_{eg} - \omega_k)$, where we used Equation (24) in the last equality. Therefore, we may simplify Equation (25) to

$$\langle g; 1_{k\sigma} 1_{k'\sigma'} | H_M^{\text{eff}}(t) | e; 0 \rangle = \frac{\hbar \sqrt{\omega_k \omega_{k'}}}{2\epsilon_0 V} e^{i(\omega_k + \omega_{k'} - \omega_{eg})t} \epsilon_{k'\sigma'}^j \epsilon_{k\sigma}^l \alpha_{jl}^{ge} (\omega_{eg} - \omega_k). \quad (26)$$

The probability rate of emitting one photon in a solid angle $d\Omega$ around \hat{k} and with a frequency in the interval $(\omega, \omega + d\omega)$ and another in a solid angle $d\Omega'$ around \hat{k}' , as well as with a frequency in the interval $(\omega', \omega' + d\omega')$, is given by (from now on we denote $\omega \equiv \omega_k$ and $\omega' \equiv \omega_{k'}$)

$$d\Gamma^{\text{TPSE}} = \frac{V^2}{(2\pi)^6} d\Omega d\Omega' d\omega d\omega' \frac{\omega^2 \omega'^2}{c^6} \frac{\left| \int_0^t dt' \langle g; 1_{k\sigma} 1_{k'\sigma'} | H_M^{\text{eff}}(t') | e; 0 \rangle \right|^2}{\hbar^2 t}. \quad (27)$$

Employing Fermi's golden rule, we arrive at

$$\frac{d\Gamma^{\text{TPSE}}}{d\Omega d\Omega' d\omega d\omega'} = \frac{\omega^3 \omega'^3}{c^6 (2\pi)^5 (2\epsilon_0)^2} \left| \epsilon_{k'\sigma'}^j \epsilon_{k\sigma}^l \alpha_{jl}^{ge} (\omega_{eg} - \omega) \right|^2 \delta(\omega_{eg} - \omega - \omega'). \quad (28)$$

Integration over the solid angles may be readily evaluated from the identity

$$\sum_{\sigma, \sigma'} \int d\Omega d\Omega' \epsilon_{k'\sigma'}^j \epsilon_{k\sigma}^{m*} \epsilon_{k'\sigma'}^{n*} \epsilon_{k\sigma}^l = \frac{(8\pi)^2}{9} \delta_{ml} \delta_{jn}. \quad (29)$$

We also integrate over ω' to find the photon emission rate:

$$\frac{d\Gamma^{\text{TPSE}}}{d\omega} = \frac{\omega^3 (\omega_{eg} - \omega)^3}{18c^6 \pi^3 \epsilon_0^2} \alpha_{jl}^{ge} (\omega_{eg} - \omega) \alpha_{jl}^{*ge} (\omega_{eg} - \omega), \quad (30)$$

which is equivalent to the result of Ref. [2].

When performing second-order perturbation theory, the usual notation is to describe the molecular response in terms not of α_{ge} —which is a function of a single frequency variable, but rather a function of two frequency variables, which are obtained from Equation (24) by replacing $\omega_{re} + \omega$ by $\omega_{rg} - \omega'$ in the second term. The calculation from the new effective Hamiltonian (11) not only yields the two-photon spontaneous emission rate with a much shorter first-order calculation but also describes the results in terms of a single frequency variable function that sheds an interesting light on the physical mechanism involved in the phenomenon. In order to unveil the physical significance of α_{jl}^{ge} , let us project the Hamiltonian H_M^{eff} into the field's Hilbert space, thus generalizing Equation (12) for situations where the molecule undergoes an internal transition. This is done by defining the new effective Hamiltonian from Equation (11):

$$H_M^{\text{eff}(ge)}(t) := \langle g | H_M^{\text{eff}}(t) | e \rangle = -\frac{1}{2} \int_{-\infty}^t dt' D_{jl}^{ge}(t, t') E_j(\mathbf{0}, t) E_l(\mathbf{0}, t'), \quad (31)$$

which involves only electric field operators. Note that $D_{jl}^{se}(t, t')$, given by Equation (20), is not a real number, and, therefore, $H_M^{\text{eff}(ge)}$ is non-Hermitian. This is due to the fact that the field degrees of freedom alone constitute an open quantum system, extracting energy from the drive provided by the molecular internal transitions encapsulated in $D_{jl}^{se}(t, t')$. The non-hermiticity of Hamiltonian (31) also reflects the break of time inversion symmetry imposed by the two-photon decay.

Following the same steps that led us from Equations (12) to (15), we obtain

$$H_M^{\text{eff}(ge)}(t) = -\frac{1}{2} \mathbf{d}^{\text{ind}(ge)}(t) \cdot \mathbf{E}(\mathbf{R}, t), \quad (32)$$

where the induced dipole for the transition $|e\rangle \rightarrow |g\rangle$ is given by

$$\mathbf{d}_j^{\text{ind}(ge)}(t) = \sum_{k\sigma} \left[\alpha_{jl}^{ge}(\omega_{eg} + \omega_k) E_{k\sigma}^{l(+)}(\mathbf{R}, t) + \alpha_{jl}^{ge}(\omega_{eg} - \omega_k) E_{k\sigma}^{l(-)}(\mathbf{R}, t) \right] e^{-i\omega_{eg}t}. \quad (33)$$

For this reason, we denominate α_{jl}^{ge} as the *transition polarizability tensor*. This is a useful concept whenever the transition dipole element of a given internal molecular transition vanishes but can be induced by an external electric field. It generalizes the concept of the polarizability tensor, which stands for the dipole induced for a fixed internal molecular state. This induced transition dipole acts as an external source oscillating with frequency ω_{eg} and driving the field appearing in the effective Hamiltonian (31). Here, $\omega_{eg} > 0$ indicates that energy-conserving processes must be accompanied by photon creation, as can be verified in Equation (14). In this case, only the last term in Equation (33) contributes to the process. The other term is relevant for two-photon absorption, and the calculation presented in the section applies with minor modifications to this case.

4. The Molecules Dress the Field

In the previous section, we investigated the convenience of employing effective Hamiltonians in which the electric field dresses the molecules. Now, we shall analyze the opposite case and present an effective Hamiltonian that describes a molecule dressing the electric field operator. Consider two nonpolar molecules A and B . The electric dipole Hamiltonian describing this system in the interaction picture is

$$H^{(2)} = H_A + H_B, \quad (34)$$

where $H_\zeta = -\mathbf{d}_\zeta(t) \cdot \mathbf{E}(\mathbf{R}_\zeta, t)$, and \mathbf{d}_ζ is the electric dipole operator of molecule $\zeta = A, B$, whose center of mass is at position \mathbf{R}_ζ . We again represent the system's state with $|\psi(t)\rangle$, satisfying Equation (4), but implicitly including a tensor product of both the molecules' and fields' states. We follow the same reasoning as in the previous section. In this case, however, we want the molecule B to dress the electric field operator. Hence, we choose as the unitary transformation the inverse of the evolution operator for the coupling between molecule B and the field:

$$U_F = \tilde{\mathcal{T}} e^{\frac{i}{\hbar} \int_{-\infty}^t dt' H_B(t')}, \quad (35)$$

where $\tilde{\mathcal{T}}$ is the anti-time ordering operator (earlier-time operators on the left). Its presence implies a crucial difference in comparison with Equation (5), and its purpose is to eliminate H_B so that the entire role played by molecule B will be through the field it produces. If only molecule B were present, the unitary transformation U_F would take the interaction picture into the Heisenberg picture. Nonetheless, in the presence of atom A , this unitary transformation yields a new effective Hamiltonian, to which we now turn our attention.

Following steps analogous to those in Section 2, the equivalent Hamiltonian is given by

$$H_F = U_F H^{(2)}(t) U_F^{-1} + i\hbar \frac{\partial U_F}{\partial t} U_F^{-1}. \quad (36)$$

Due to the anti-time ordering operator, we have $i\hbar\partial_t U_F = -U_F H_B$, and, thus,

$$H_F = -\mathbf{d}_A(t) \cdot U_F \mathbf{E}(\mathbf{R}_A, t) U_F^{-1}, \quad (37)$$

canceling H_B as anticipated. Expanding up to the linear term in \mathbf{d}_B , we obtain (see Appendix A)

$$U_F \mathbf{E}(\mathbf{R}_A, t) U_F^{-1} \approx \mathbf{E}(\mathbf{R}_A, t) + \mathbf{E}_{\text{dip},B}(\mathbf{R}_A, t), \quad (38)$$

where

$$\begin{aligned} \mathbf{E}_{\text{dip},B}(\mathbf{R}_A, t) = \frac{1}{4\pi\epsilon_0} \left\{ \frac{3[\hat{\mathbf{r}} \cdot \mathbf{d}_B(t_r)]\hat{\mathbf{r}} - \mathbf{d}_B(t_r)}{r^3} + \frac{3[\hat{\mathbf{r}} \cdot \dot{\mathbf{d}}_B(t_r)]\hat{\mathbf{r}} - \dot{\mathbf{d}}_B(t_r)}{cr^2} \right. \\ \left. + \frac{[\hat{\mathbf{r}} \cdot \ddot{\mathbf{d}}_B(t_r)]\hat{\mathbf{r}} - \ddot{\mathbf{d}}_B(t_r)}{c^2 r} \right\}, \end{aligned} \quad (39)$$

with $\mathbf{r} = \mathbf{R}_A - \mathbf{R}_B$ and $t_r = t - r/c$ being the retarded time. This expression corresponds to the electric field generated by dipole B at the position of molecule A . This result is readily extended to any number of molecules by exchanging $H_B \rightarrow H_B + H_C + \dots$ in Equation (35), thus obtaining

$$H_F^{\text{eff}} = -\mathbf{d}_A(t) \cdot \left[\mathbf{E}(\mathbf{R}_A, t) + \sum_{\zeta=B,C,\dots} \mathbf{E}_{\text{dip},\zeta}(\mathbf{R}_A, t) \right]. \quad (40)$$

While Equation (37) is exact and constitutes an equivalent Hamiltonian, Equation (40) is effective and valid only up to linear order in \mathbf{d}_B , \mathbf{d}_C , etc. It is worth mentioning that Equation (40) can be generalized to other situations. For instance, if atom A is in the presence of a magnetically polarizable atom [30,31], we have to add the electric field produced by the magnetic dipole of atom B in Equation (38). In the next section, we demonstrate the convenience of the new effective Hamiltonian H_F^{eff} by obtaining the RET rate in a first-order calculation.

5. Application to the Resonance Energy Transfer

In a resonance energy transfer (RET) process, an excited molecule decays through nonradiative channels, transferring its energy to a molecule in the ground state [32–41]. This phenomenon is of notable importance to many areas of science due to its broad range of applications across fields such as chemistry [42], medicine [43], and biology [44]. Throughout this section, we discuss the probability that an excited molecule A decays, exciting an identical molecule B that was initially in its ground state, placed at a distance r from A , with both in vacuum.

Up to the second order in perturbation theory, the probability amplitude of interest can be calculated as [15]

$$\mathcal{M}_{fi} \approx \langle \psi_f | H_{\text{int}} | \psi_i \rangle + \lim_{\eta \rightarrow 0^+} \sum_r \frac{\langle \psi_f | H_{\text{int}} | \psi_r \rangle \langle \psi_r | H_{\text{int}} | \psi_i \rangle}{E_i - E_r + i\eta}. \quad (41)$$

In this expression, $|\psi_i\rangle = |e_A, g_B, 0_{k\sigma}\rangle$ (with energy E_i) and $|\psi_f\rangle = |g_A, e_B, 0_{k\sigma}\rangle$ describe, respectively, the system's initial and final states, \hat{H}_{int} is the interaction Hamiltonian, and $|\psi_r\rangle$ are the intermediate states with energy E_r . In the standard approach, the interaction Hamiltonian is taken as the dipolar Hamiltonian given by Equation (34): $H_{\text{int}} = H^{(2)}$. With this choice, however, the first term in Equation (41) vanishes, and the RET rate is obtained from second-order perturbation theory. Here, we offer an alternative and simpler

approach by letting atom B dress the field and taking $H_{\text{int}} = H_{\text{F}}^{\text{eff}}$, as in Equation (40). In this case, it suffices to calculate the first-order matrix element

$$\mathcal{M}_{fi} = -\langle g_A | \mathbf{d}_A(t) | e_A \rangle \cdot \langle e_B | \mathbf{E}_{\text{dip},B}(\mathbf{R}_A, t) | g_B \rangle. \quad (42)$$

Following Equation (21), the first matrix element on the right-hand side of the previous equation becomes (more precisely, we should consider the evolution beginning at time t_0 ; however, as explained in Section 3, this would only contribute as an irrelevant global phase)

$$\langle g_A | \mathbf{d}_A(t) | e_A \rangle = e^{-i\omega_{eg}t} \mathbf{d}_A^{ge}, \quad (43)$$

and, by using Equation (39), the terms contained in the second matrix element give the contributions

$$\langle e_B | \mathbf{d}_B(t_r) | g_B \rangle = e^{i\omega_{eg}t} e^{-ikr} \mathbf{d}_B^{eg}, \quad (44)$$

$$\begin{aligned} \langle e_B | \partial_t \mathbf{d}_B(t_r) | g_B \rangle &= \frac{\partial}{\partial t} \langle e_B | \mathbf{d}_B(t_r) | g_B \rangle = i\omega_{eg} e^{i\omega_{eg}t} e^{-ikr} \mathbf{d}_B^{eg}, \\ \langle e_B | \partial_t^2 \mathbf{d}_B(t_r) | g_B \rangle &= \frac{\partial^2}{\partial t^2} \langle e_B | \mathbf{d}_B(t_r) | g_B \rangle = -\omega_{eg}^2 e^{i\omega_{eg}t} e^{-ikr} \mathbf{d}_B^{eg}, \end{aligned} \quad (45)$$

where $k = \omega_{eg}/c$. Replacing these results in Equation (42), we arrive at

$$\mathcal{M}_{fi} = \frac{d_{i,A}^{ge} d_{j,B}^{eg} e^{-ikr}}{4\pi\epsilon_0 r^3} \left[(\delta_{ij} - 3\hat{r}_i \hat{r}_j)(1 + ikr) - (\delta_{ij} - \hat{r}_i \hat{r}_j)k^2 r^2 \right]. \quad (46)$$

By applying Fermi's golden rule,

$$\Gamma^{\text{RET}} = \frac{2\pi}{\hbar^2} \rho(\omega_f) |\mathcal{M}_{fi}|^2, \quad (47)$$

where $\rho(\omega_f)$ is the density of final states with energy $E_f = \hbar\omega_f$, and we directly recover the well-known result for the RET rate [45,46].

6. The Dressed Molecules Dress the Field—And the Reverse

The first-order perturbation in the Hamiltonian (40) vanishes whenever the electric dipole operator of one of the molecules cannot connect the involved molecular states. An example is the force between molecules in their ground state to be analyzed in the next section. Here, instead, we focus on a general discussion without specifying the molecular internal state. The physical mechanism that limits the dipole–dipole correlation depends strongly on the distance R separating the molecules. Indeed, two characteristic time scales are key to understanding the two different regimes: the time it takes light to travel between the molecules, $t_\gamma = r/c$, and the characteristic time for dipole fluctuations, $t_d = 1/\omega_0$, where ω_0 is a typical transition frequency for the molecules. In the asymptotic long-distance regime, $t_\gamma \gg t_d$, it is the electrodynamical retardation that limits the dipole–dipole correlation, and we may neglect dispersion in the atomic response. In the opposite short-distance regime, electrodynamical retardation is negligible, and it is now the delay in the molecular response that limits the dipole–dipole correlation. Now, the molecular dispersion is crucial, but we can take the electrostatic limit for the electric field produced by each electric dipole. To go deeper into the physical particularities of these two complementary regimes, we shall develop a different effective Hamiltonian appropriate to each case.

6.1. The Dressed Molecules Dress the Field: Retarded Long-Distance Regime

In the long-distance regime, we may neglect dispersion in the molecules, which is tantamount to considering an instantaneous molecular response. This means that the time-

scale variation for the electric field is much slower than the molecular response, enabling us to approximate

$$\frac{i}{\hbar} \int_{-\infty}^t dt' [d_j(t), d_l(t')] E_l(\mathbf{R}, t') \approx \Pi_{jl} E_l(\mathbf{R}, t), \quad (48)$$

when evaluating the effective Hamiltonian $H_M^{\text{eff}}(t)$ given by Equation (11). We have defined the molecular operator Π_{jl} as

$$\Pi_{jl} = \frac{i}{\hbar} \int_{-\infty}^{\infty} dt' \theta(t - t') [d_j(t), d_l(t')]. \quad (49)$$

From Equation (13), we see that the expectation value $\langle g | \Pi_{jl} | g \rangle$ is the static polarizability of the molecule in its ground state, given by setting $\omega = 0$ in Equation (18). The tensor operator Π_{jl} generalizes this concept by enabling us to capture the static response even for processes involving changes in the molecular internal state. Substituting (48) into (11) leads to

$$H_M^{\text{eff},s}(t) = -\frac{1}{2} \Pi_{jl} E_j(\mathbf{R}, t) E_l(\mathbf{R}, t), \quad (50)$$

which corresponds to the static response limit of $H_M^{\text{eff}}(t)$.

In the case of two molecules, dipole–dipole correlations arise in second-order perturbation theory in the Hamiltonian

$$H_M^{\text{eff},s(2)}(t) = H_{M,A}^{\text{eff},s(2)}(t) + H_{M,B}^{\text{eff},s(2)}(t) = -\frac{1}{2} \Pi_{A,jl} E_j(\mathbf{R}_A, t) E_l(\mathbf{R}_A, t) - \frac{1}{2} \Pi_{B,jl} E_j(\mathbf{R}_B, t) E_l(\mathbf{R}_B, t), \quad (51)$$

where $\Pi_{\zeta,jl}$ is the operator (49) for molecule $\zeta = A, B$.

An equivalent Hamiltonian where the molecules couple directly with each other will be able to capture the dipole–dipole correlation in first-order perturbation theory. This can be done by employing the unitary transformation

$$U_{\text{MF}} = \tilde{T} e^{\frac{i}{\hbar} \int_{-\infty}^t dt' H_{M,B}^{\text{eff},s}(t')}, \quad (52)$$

which mimics the one employed in Section 4, with the difference that it is the dressed molecule (through operator Π_{jl}), instead of the naked molecule, that dresses the field. Following the same steps that led us from Equation (34) for molecule B into Equation (37), we get

$$H_{\text{MF}}^{\text{eff},s}(t) = U_{\text{MF}} H_{M,A}^{\text{eff},s}(t) U_{\text{MF}}^{-1}. \quad (53)$$

$H_{\text{MF}}^{\text{eff},s}$ is very suitable for handling effects related to the interaction between atoms A and B because the expansion of U_{MF} in Equation (53) contains terms combining the product $\Pi_{A,jl} \Pi_{B,mn}$. Such terms also appear through a fourth-order perturbation theory in Hamiltonian (34) but already appear in first order here. To obtain $H_{\text{MF}}^{\text{eff},s}$, it is enough to implement the transformation rule for the electric field at \mathbf{R}_A , since $\Pi_{A,jl}$ commutes with $\Pi_{B,mn}$. Substituting Equation (50) into (52), we obtain the following up to linear order in Π_B (see Appendix A):

$$U_{\text{MF}} E(\mathbf{R}_A, t) U_{\text{MF}}^{-1} \approx E(\mathbf{R}_A, t) + E_{\text{dip},B}^{\text{ind}}(\mathbf{R}_A, t), \quad (54)$$

where $E_{\text{dip},B}^{\text{ind}}(\mathbf{R}_A, t)$ is given by Equation (39) with the substitution $d_{B,j}(t_r) \rightarrow \Pi_{B,jk} E_k(\mathbf{R}_B, t_r)$. This result is mathematically similar to Equation (38) but with a remarkable physical difference. Here, the field is dressed not by a naked molecule but by a dressed one. This means that the source of the electric dipole field is not the molecular dipole operator but rather a vacuum-induced dipole—as indicated by the superscript “ind” in Equation (54). From Equations (53) and (54), we arrive at

$$H_{\text{MF}}^{\text{eff},s}(t) = -\frac{1}{2} \Pi_{A,jk} \left(E_k(\mathbf{R}_A, t) E_{\text{dip},B,j}^{\text{ind}}(\mathbf{R}_A, t) + E_{\text{dip},B,k}^{\text{ind}}(\mathbf{R}_A, t) E_j(\mathbf{R}_A, t) \right), \quad (55)$$

where we have kept only the terms capturing the dipole–dipole correlation and neglected the higher-order term $\Pi_{A,jk} E_{\text{dip},B,k}^{\text{ind}}(\mathbf{R}_A, t) E_{\text{dip},B,j}^{\text{ind}}(\mathbf{R}_A, t)$. This expression is manifestly symmetric upon the exchange $A \longleftrightarrow B$, as can be verified by substituting Equation (39) into (55).

As an application of the effective Hamiltonian (55), we may consider that both molecules are at their ground states throughout the entire process. In this case, we may take the expectation value of $H_{\text{MF}}^{\text{eff},s}(t)$ in the ground states of the molecules, which is equivalent to substituting the operators Π_{jl} with the static polarizability tensor of the corresponding molecule in Equation (55). In the particular case of isotropic molecules, this reproduces the asymptotic long-distance limit of the effective Hamiltonian originally employed by P.W. Milonni, which readily yields the known Casimir–Polder result in first order [18]. For comparison, when taking the average of $H_{\text{M}}^{\text{eff},s(2)}$ (see Equation (51)) over the molecular ground state, the resulting effective Hamiltonian [47] yields the Casimir–Polder energy only to the second order of perturbation theory.

In the opposite short-distance limit, molecular dispersion is essential, and we cannot make the approximation given by Equation (48). In this case, it is more convenient to work with a different effective Hamiltonian, which we shall present in the next subsection.

6.2. The Dressed Field Dresses the Molecules: Non-Retarded Regime

We now turn to the opposite regime, in which the intermolecular distance is so small that we may neglect the electromagnetic retardation in comparison to the molecular response time. Unlike the other examples in this paper, this case does not require quantization of the electromagnetic field. On the other hand, the molecular dispersion is crucial in this regime. The dipole–dipole correlation is usually obtained from a second-order perturbation theory in the dipole–dipole Hamiltonian [48]

$$H_{dd} = \frac{d_{A,j} d_{B,k} (\delta_{jk} - 3\hat{r}_j \hat{r}_k)}{4\pi\epsilon_0 r^3}, \quad (56)$$

where $\mathbf{r} = r\hat{\mathbf{r}}$ is the position of molecule B with respect to molecule A . Notice that this Hamiltonian is a particular case of Equation (40) without the vacuum electric field operator and with the dipole electric field taken in the electrostatic approximation. In the non-retarded regime, the field and the molecular operators switch roles with respect to what happens in the retarded asymptotic regime. While, in the latter, we could begin with Hamiltonian (48), which approximates the molecular response with its dressed static response, Equation (56) is precisely the opposite: now it is the field that is dressed by its static response. Indeed, the electrostatic dipole field leading to (56) corresponds to the zero-frequency limit of the Green function of the wave equation, which plays the role of the field susceptibility, as discussed in Appendix B.

Mirroring the procedure of the previous subsection, we let the already-dressed field dress the molecules, thus leading to a new effective Hamiltonian. In the long-distance regime, we employed a unitary transformation extending the formalism of Section 4. Here, on the other hand, we want to extend the formalism developed in Section 2. As a first step, we write Hamiltonian (56) in the interaction picture and then take as the unitary transformation the operator

$$U_{\text{FM}} = \exp\left(\frac{i}{\hbar} \int_{-\infty}^t dt' H_{dd}(t')\right), \quad (57)$$

which should be compared to Equation (5). Following steps analogous to the ones leading to Equation (10) yields

$$H_{\text{FM}}^{\text{eff}}(t) = -\frac{i}{2\hbar} \int_{-\infty}^t dt' [H_{dd}(t), H_{dd}(t')]. \quad (58)$$

Since operators involving different molecules commute, we have

$$[d_{A,j}(t)d_{B,k}(t), d_{A,m}(t')d_{B,n}(t')] = \frac{[d_{A,j}(t), d_{A,m}(t')]\{d_{B,k}(t), d_{B,n}(t')\}}{2} + \frac{\{d_{A,j}(t), d_{A,m}(t')\}[d_{B,k}(t), d_{B,n}(t')]}{2}. \quad (59)$$

By substituting Equation (56) and the previous identity into Equation (58), we obtain the effective Hamiltonian

$$H_{\text{FM}}^{\text{eff}} = -\frac{i(\delta_{jk} - 3\hat{r}_j\hat{r}_k)(\delta_{mn} - 3\hat{r}_m\hat{r}_n)}{64\hbar\pi^2\epsilon_0^2r^6} \int_{-\infty}^t dt' ([d_{A,j}(t), d_{A,m}(t')]\{d_{B,k}(t), d_{B,n}(t')\} + \{d_{A,j}(t), d_{A,m}(t')\}[d_{B,k}(t), d_{B,n}(t')]). \quad (60)$$

The new effective Hamiltonian (60) has two terms that capture the physics involved in the dipole–dipole correlation. The product $[d_{A,j}(t), d_{A,m}(t')]\{d_{B,k}(t), d_{B,n}(t')\}$ measures how the dipole fluctuations of molecule *B* induces a dipole in molecule *A*, while the other term is its reciprocal. This decomposition is possible because, differently from the standard approach based on second-order perturbation theory with the time-independent dipole–dipole Hamiltonian (56) where the two molecules are considered as an isolated system, here, we take the complementary approach of considering each molecule separately as an open quantum system. This perspective offers two main novelties: (i) $H_{\text{FM}}^{\text{eff}}$ brings to light the dynamical character of the dispersion interaction by making an explicit connection with dipole fluctuations, and (ii) $H_{\text{FM}}^{\text{eff}}$ enables us to assess the contribution from the fluctuations of each molecule separately. In the next section, we analyze an example that illustrates these advantages.

7. Application to the London Interaction Energy

In this section, we consider the dispersion interaction between two ground-state non-polar molecules *A* and *B* in vacuum, which interact due to correlations between their fluctuating electric dipoles. As discussed in the previous section, the physical mechanism limiting the dipole–dipole correlation strongly depends on comparing the distance separating the molecules and their internal transition wavelengths. For ground-state molecules, the resulting intermolecular interaction energy exhibits a different power-law dependence with distance in each of the two regimes discussed in Section 6.

As originally demonstrated by London [49], the non-retarded interaction energy can be obtained without quantizing the electromagnetic field and scales with $1/r^6$. The asymptotic long-distance limit was first obtained in the seminal paper by Casimir and Polder [50], where they showed that retardation imposes the necessity of quantizing the electromagnetic field and demonstrated that the interaction energy scales asymptotically with $1/r^7$.

Both regimes have still been at the center of intense investigation in recent years. Casimir–Polder forces have been studied considering excited [51–56] and chiral [57–60] particles. The influence of neighboring surfaces with ever-increasing complexity [61–73] and with dynamical [74–76] and thermal effects [77–83] has also been considered.

The force in the non-retarded regime—sometimes referred to as London or van der Waals force—plays a pivotal role in chemistry [84] and condensed matter physics, where short-range interactions prevail. In van der Waals heterostructures, two-dimensional materials are stacked and held together by London dispersion forces, generating materials with fascinating physical properties that are useful for designing new electronic devices [85–87]. Density functional theory provides a powerful framework capable of obtaining increasingly precise descriptions of molecular polarizabilities and London dispersion forces [88–90]. Modifications of the force due to an intervening electrolyte medium [91–93], with the atomic motion in connection with quantum friction [94–105] or with non-local interferometric phases [106–108], the atomic internal state [109], and coming from boundary conditions im-

posed by nearby structures [110–114], have disclosed important features of the London–van der Waals interactions.

In the previous section, we discussed how the Casimir–Polder result for the asymptotic long-distance limit can be derived from the effective Hamiltonian $H_{\text{MF}}^{\text{eff}}$ (55). In this section, we obtain the London result for the short-distance non-retarded limit from the new effective Hamiltonian $H_{\text{FM}}^{\text{eff}}$ (60), which provides new physical insights into the dipole–dipole correlation present in the non-retarded regime. By taking the average of Hamiltonian (60) in the ground state of the molecules and employing the result (13) for the molecular polarizability tensors $\alpha_{jl}^A, \alpha_{jl}^B$, we obtain

$$E_{\text{London}} = -\frac{\hbar(\delta_{jk} - 3\hat{r}_j\hat{r}_k)(\delta_{mn} - 3\hat{r}_m\hat{r}_n)}{64\pi^2\epsilon_0^2r^6} \int_{-\infty}^{\infty} d\tau \left(\alpha_{jm}^A(\tau)\eta_{kn}^B(\tau) + \eta_{jm}^A(\tau)\alpha_{kn}^B(\tau) \right), \quad (61)$$

where we defined the symmetrical dipole correlation function

$$\eta_{jm}^{\zeta}(\tau) := \frac{1}{\hbar} \langle g | \left\{ d_j^{\zeta}(t' + \tau), d_m^{\zeta}(t') \right\} | g \rangle, \quad (62)$$

with $\zeta = A, B$. To work in the Fourier space, we can apply Parseval's theorem, so Equation (61) becomes

$$E_{\text{London}} = -\frac{\hbar(\delta_{jk} - 3\hat{r}_j\hat{r}_k)(\delta_{mn} - 3\hat{r}_m\hat{r}_n)}{128\pi^3\epsilon_0^2r^6} \int_{-\infty}^{\infty} d\omega \left(\alpha_{jm}^A(\omega)\eta_{kn}^B(\omega) + \eta_{jm}^A(\omega)\alpha_{kn}^B(\omega) \right), \quad (63)$$

where we used that $\eta^{A,B}(\omega)$ are real functions, as they are Fourier transforms of real even functions. This result is the analog for two molecules of the decomposition obtained for an atom coupled to the vacuum electric field [115–117]. In the latter, the field susceptibility captures the field radiation reaction. More recently, an analogous decomposition was also obtained for atoms interacting with a scalar quantum field [118]. A decomposition similar to (63) was employed to derive a nonlocal phase for a moving atom interacting with a planar surface [119] and a Sagnac-like atomic phase induced by a rotating nanosphere [120].

In the isotropic case, the polarizability tensors simplify to $\alpha_{rs}^{A(B)}(\tau) = \delta_{rs}\alpha^{A(B)}(\tau)$, and the symmetric correlation functions simplify to $\eta_{rs}^{A(B)}(\tau) = \delta_{rs}\eta^{A(B)}(\tau)$. Then, Equation (63) leads to

$$E_{\text{London}} = -\frac{3\hbar}{64\pi^3\epsilon_0^2r^6} \int_{-\infty}^{\infty} d\omega \left(\alpha^A(\omega)\eta^B(\omega) + \eta^A(\omega)\alpha^B(\omega) \right). \quad (64)$$

In Appendix B, we employ the analytical properties of the correlation functions to demonstrate that our results are equivalent to the standard way of expressing the London interaction energy for any molecular model of the polarizabilities. Here, we show the convenience of Equation (64) by considering the simple case of two-level atoms, for which ($\zeta = A, B$) [18]

$$\alpha^{\zeta}(\omega) = \frac{\alpha_0^{\zeta}\omega_{0\zeta}^2}{\omega_{0\zeta}^2 - \omega^2}, \quad (65)$$

$$\eta^{\zeta}(\omega) = \pi\alpha_0^{\zeta}\omega_{0\zeta} [\delta(\omega - \omega_{0\zeta}) + \delta(\omega + \omega_{0\zeta})]. \quad (66)$$

Let us analyze each contribution to the London interaction energy in Equation (64) separately. We define

$$E_{\text{London}}^{A \rightarrow B} = -\frac{3\hbar}{64\pi^3\epsilon_0^2r^6} \int_{-\infty}^{\infty} d\omega \eta^A(\omega)\alpha^B(\omega), \quad (67)$$

as the contribution arising from the dipole induced at atom B by the dipole fluctuations of atom A . From Equations (65) and (66), we obtain

$$E_{\text{London}}^{A \rightarrow B} = -\frac{3\hbar\alpha_0^A\alpha_0^B\omega_{0A}\omega_{0B}}{32\pi^2\epsilon_0^2r^6}\frac{\omega_{0B}}{\omega_{0B}^2 - \omega_{0A}^2}. \quad (68)$$

The interaction energy is $E_{\text{London}} = E_{\text{London}}^{B \rightarrow A} + E_{\text{London}}^{A \rightarrow B}$, with $E_{\text{London}}^{B \rightarrow A}$ being obtained by interchanging the roles of A and B in Equation (68).

Let us consider $\omega_{0A} > \omega_{0B}$. In that case, from Equation (68), we see that $E_{\text{London}}^{A \rightarrow B} > 0$, indicating that the dipole induced at a slower atom by a faster one generates a repulsive contribution to the dispersion force. This is due to the fact that the polarizability given by Equation (65) becomes negative for frequencies higher than the atomic transition frequency. Indeed, the induced dipole at the slower atom B cannot follow the fast oscillation of the fluctuating dipole of atom A . The induced dipole at B lags behind the field of atom A and points opposite to its direction at a given time. As a consequence, the induced dipole at B repels the fluctuating dipole at A . However, the opposite holds for the complementary term $E_{\text{London}}^{B \rightarrow A}$: the dipole induced in the faster atom A can follow the dipole fluctuations of atom B in phase, leading to an attractive contribution. Attraction overcomes repulsion by a factor ω_{0A}/ω_{0B} , since the slower atom couples less effectively to the field than the faster one. If $\omega_{0A} = \omega_{0B}$, each contribution diverges due to a resonant response. This divergence would be avoided if dissipation were taken into account. Nevertheless, it is remarkable that the divergence cancels once we sum $E_{\text{London}}^{B \rightarrow A}$ and $E_{\text{London}}^{A \rightarrow B}$, leaving us with the well-behaved total interaction energy

$$E_{\text{London}} = -\frac{3\hbar\alpha_0^A\alpha_0^B}{32\pi^2\epsilon_0^2r^6}\frac{\omega_{0A}\omega_{0B}}{\omega_{0A} + \omega_{0B}}, \quad (69)$$

which agrees with the result [2] calculated from second-order perturbation theory based on the dipole–dipole Hamiltonian (56).

Notice that varying ω_{0B} while keeping the other parameters fixed shows that the attraction is maximal when $\omega_{0B} \rightarrow \infty$. The previous decomposition clearly illustrates the physical mechanism involved. From Equation (68), we see that in this limit, the repulsive contribution $E_{\text{London}}^{B \rightarrow A}$ vanishes, indicating that atom A is effectively transparent, decoupling from the rapid oscillating field produced by B . The attractive term in Equation (68), on the other hand, takes its maximal absolute value in this limit, since the response of atom B is so fast that it perfectly mirrors the fluctuations of the other atom. In this sense, we may conclude that atom B in the limit $\omega_{0B} \rightarrow \infty$ is the atomic analog of a perfect conductor.

As was true with the other effective Hamiltonians discussed in this paper, we see that the convenience of employing $H_{\text{FM}}^{\text{eff}}$ is twofold: (i) it lowers the perturbation order required to obtain the London dispersion energy from second to first order, and (ii) it offers physical insights into the mechanisms involved in the phenomenon. The results in this section can be readily extended for multilevel atoms. To this end, it suffices to substitute Equations (65) and (66) with a summation over all internal transition frequencies.

8. Final Remarks and Conclusions

All phenomena in molecular quantum electrodynamics can be obtained from the multipolar Hamiltonian. In this paper, we restricted our attention to phenomena that can be treated perturbatively (which includes the vast majority of cases in this field). In most situations, the dominant effect is obtained from a high-order perturbation theory, requiring intermediate states to connect the initial and the final states. A clear example is the interatomic interaction. While in classical electrodynamics, we may always take the field at each charged particle as the superposition of the field generated by all other particles, in standard quantum electrodynamics, each particle couples only to the free electromagnetic field. Consequently, we must go up to the fourth order to obtain the dominant contribution when considering molecules without permanent electric dipole moments. An alternative

is to build effective Hamiltonians. They are customized for each specific application and lose meaning and validity after some point in the perturbative expansion. Not only do they greatly simplify the technical difficulties involved in calculations using the multipolar Hamiltonian, but, equally importantly, the effective Hamiltonians cast the phenomena in a new light, offering insightful physical interpretations.

Several effective Hamiltonians have successfully been employed by many authors in the last decades. In this paper, we have developed a systematic approach to constructing effective Hamiltonians, which allowed us to derive a number of new ones, choosing as a unitary transformation the Hermitian conjugate of the evolution operator for part of the system. This transfers part of the time evolution from the vector state to the operators, dressing them and providing a Hamiltonian that requires a lower order in perturbation theory to account for the process of interest. This method can always be used when the first-order perturbation theory vanishes. Our approach yields time-dependent Hamiltonians that enable us to follow the energy exchange between matter and the field, with each subsystem constituting an open quantum system. We emphasize here that our system of interest is the entire molecule–field system, and it is not interesting to trace over any of the subsystems, as is common in an open quantum system approach [121–123].

As a first application, we have derived the Hamiltonian H_M^{eff} , where the field dresses the molecule and the dipole operators are replaced by their commutator at different times. If we project the commutator in an internal molecular state, it yields the dynamical polarizability of the molecule for the corresponding state. Its nondiagonal elements, on the other hand, allow the dressing to leave the molecule in a final state that is different from the initial one. We have demonstrated that this new time-dependent Hamiltonian provides a simpler treatment of the two-photon spontaneous emission, as the dominant contribution is obtained in first-order perturbation theory. In addition, our formalism introduces the concept of an induced dipole transition, which generalizes the notion of an induced dipole for a given internal state.

Then, we discussed applications involving two molecules A and B . We constructed the new effective Hamiltonian H_F^{eff} through a unitary transformation that transfers all of the effects related to molecule B to the electric field it generates. In this way, molecule A feels an effectively dressed electric field given by the superposition of the free vacuum electric field, and the one generated by the dipole operator of molecule B . H_F^{eff} allows for the description of the resonance energy transfer rate in first-order perturbation theory.

Lastly, we derived two additional Hamiltonians that merge aspects of the previous two, where each one is appropriate for a different intermolecular distance regime. In the asymptotic long-distance regime, molecular dispersion is negligible, enabling us to derive an effective Hamiltonian H_{MF}^{eff} which is formally similar to H_M^{eff} . In this new case, however, the field acting on molecule A is given by the superposition of the free electric field and the one produced by the vacuum-induced dipole generated on molecule B . When we average H_{MF}^{eff} over the molecular ground state, we re-obtain the asymptotic limit of the Hamiltonian employed by P. Milonni [18].

Finally, for the short-distance non-retarded limit, we derived our fourth and last effective Hamiltonian H_{FM}^{eff} based on the fact that, in this limit, we do not need to quantize the electric field. This effective Hamiltonian enables us to clearly identify the different physical mechanisms involved in the correlations responsible for the interaction, separating one term where the dipole fluctuations of molecular A induce a dipole on molecule B and another term where the roles are exchanged.

As a final application, we employed H_{FM}^{eff} to obtain the London dispersion interaction energy in first-order perturbation theory. We showed that, for two-level atoms, the dipole fluctuations of the atom with the higher transition frequency give rise to a repulsive term, since its fast fluctuations cannot be followed by the slower atom. Nonetheless, the force between two isotropic atoms is always attractive, since the fluctuations of the slower atom are strongly correlated and easily followed by the faster atom, overcoming the repulsive

contribution. The possibility of quantitatively and separately analyzing the contributions arising from each mechanism correlating fluctuating systems is an advantage of $H_{\text{FM}}^{\text{eff}}$.

The Hamiltonians presented in this paper can be employed in a great variety of situations. For instance, one may treat the effects of boundaries in the two-photon spontaneous emission or resonance energy transfer by simply introducing the appropriate field modes. As in the examples discussed in this paper, these effective Hamiltonians allow for a direct first-order calculation within perturbation theory. More notably, the methodology introduced here can be applied to generate other effective Hamiltonians that may optimize calculations and provide physical intuition.

Author Contributions: Conceptualization, C.F., P.A.M.N. and R.d.M.e.S.; Methodology, A.S.S., P.H.P. and P.P.A.; Validation, P.P.A., C.F. and P.A.M.N.; Formal analysis, A.S.S., P.H.P., C.F. and R.d.M.e.S.; Investigation, A.S.S. and P.H.P.; Writing—original draft, P.P.A., C.F., P.A.M.N. and R.d.M.e.S.; Writing—review & editing, P.P.A., C.F., P.A.M.N. and R.d.M.e.S.; Supervision, R.d.M.e.S.; Project administration, R.d.M.e.S. All authors have read and agreed to the published version of the manuscript.

Funding: This research was funded by the Brazilian agencies CAPES and CNPq. P.A.M.N. was also supported by Instituto Nacional de Ciência e Tecnologia de Fluidos Complexos (INCT-FCx) and the Research Foundations of the States of Rio de Janeiro (FAPERJ) (210.077/2023 and 201.126/2021) and São Paulo (FAPESP).

Data Availability Statement: The original contributions presented in the study are included in the article, further inquiries can be directed to the corresponding author/s.

Acknowledgments: The authors thank François Impens for enlightening discussions.

Conflicts of Interest: The authors declare no conflicts of interest.

Appendix A. Susceptibilities

Appendix A.1. Molecular Polarizability

Let us find the time evolution of the expected value of the dipole operator in the atomic state $|\phi(t)\rangle$, as determined by the electric dipole interaction Hamiltonian $H(t)$ given by Equation (3). We operate in the interaction picture, so $|\phi(t)\rangle \approx \left(\mathbb{I} - \frac{i}{\hbar} \int_{-\infty}^t dt' H(t') \right) |\phi(-\infty)\rangle$. This implies that, up to the second order in the dipole operator,

$$\langle d(t) \rangle_t = \left\langle d(t) - \frac{i}{\hbar} \int_{-\infty}^t dt' [d(t), H(t')] \right\rangle_{-\infty}, \quad (\text{A1})$$

where $\langle \mathcal{O} \rangle_t = \langle \phi(t) | \mathcal{O} | \phi(t) \rangle$. All of the electric field contributions to the molecular electric dipole are contained in the second term on the right-hand side of Equation (A1). Therefore, we refer to this term as the induced dipole $\langle d^{\text{ind}}(t) \rangle_t$, whose components can be written as

$$\langle d_j^{\text{ind}}(t) \rangle_t = \frac{i}{\hbar} \int_{-\infty}^t dt' \langle [d_j(t), d_l(t')] \rangle_{-\infty} E_l(t') =: \int_{-\infty}^t dt' \alpha_{jl}(t - t') E_l(t'), \quad (\text{A2})$$

where α_{jl} are the elements of the dynamical molecular electric polarizability tensor for the molecular state $|\phi(-\infty)\rangle$. We assume here that $|\phi(-\infty)\rangle$ is an eigenstate of the free molecular Hamiltonian H_0 , a situation where time translation symmetry ensures that the average value of $[d(t), d(t)']$ is a function of t, t' only through the difference $t - t'$, as in the last equality.

For many applications, we are interested in the situation where $|\phi(-\infty)\rangle$ is the ground state, in which case the dynamical polarizability reduces to Equation (13). This expression is still valid regardless of whether there is dissipation or not [124]. If there is no dissipation,

the polarizability can be directly expressed in terms of the eigenstates $|r\rangle$ of H_0 . Inserting a closure relation $\mathbb{I} = \sum_r |r\rangle\langle r|$ into Equation (13), we obtain the familiar expression

$$\alpha_{jl}(t-t') = \frac{2}{\hbar} \theta(t-t') \sum_r d_j^{gr} d_l^{rg} \sin[\omega_{rg}(t-t')]. \quad (\text{A3})$$

In Fourier space, the above expression immediately translates to Equation (18).

Appendix A.2. The Field of a Dipole Is the Field Susceptibility

From the expression of the quantized electric field, it is straightforward to show that (see Section 2.8 of Ref. [18])

$$\frac{i}{\hbar} \theta(t-t') [E_j(\mathbf{r}, t), E_l(\mathbf{r}', t')] = \frac{1}{\epsilon_0} \mathcal{D}_{jl} \mathcal{G}_r(|\mathbf{r}-\mathbf{r}'|, t-t'), \quad (\text{A4})$$

where \mathcal{G}_r is the retarded Green function of the wave equation, and \mathcal{D}_{jl} is the differential operator

$$\mathcal{D}_{jl} = \partial_j \partial'_l - \frac{\delta_{jl}}{c^2} \partial_t \partial'_t. \quad (\text{A5})$$

On the other hand, from Maxwell's equation, the electric field generated by a charge density ρ and electric current density \mathbf{J} is given by

$$\left(\nabla^2 - \frac{1}{c^2} \frac{\partial^2}{\partial t^2} \right) \mathbf{E} = \frac{\nabla \rho}{\epsilon_0} + \frac{1}{\epsilon_0 c^2} \partial_t \mathbf{J}. \quad (\text{A6})$$

As a source, let us consider a point dipole \mathbf{d} existing only at time t' placed at \mathbf{r}' , such that [125,126]

$$\rho(\mathbf{r}, t) = -\mathbf{d} \cdot \nabla \delta(\mathbf{r}-\mathbf{r}') \delta(t-t'), \quad (\text{A7})$$

$$\mathbf{J}(\mathbf{r}, t) = \mathbf{d} \delta(\mathbf{r}-\mathbf{r}') \partial_t \delta(t-t'). \quad (\text{A8})$$

From Equation (A6) and after integrating by parts, the electric field generated by this point dipole is

$$E_{\text{dip},j}(\mathbf{r}, t) = -\frac{d_l}{\epsilon_0} \left(\partial_j \partial'_l - \frac{\delta_{jl}}{c^2} \partial_t^2 \right) \mathcal{G}_r(|\mathbf{r}-\mathbf{r}'|, t-t') = \frac{d_l}{\epsilon_0} \mathcal{D}_{jl} \mathcal{G}_r(|\mathbf{r}-\mathbf{r}'|, t-t'), \quad (\text{A9})$$

where we used $\partial_l = -\partial'_l$ and $\partial_t = -\partial'_t$ because \mathcal{G}_r depends only on the differences $\mathbf{r}-\mathbf{r}'$ and $t-t'$. Comparing this result with Equation (A4), one can see that

$$E_{\text{dip}}(\mathbf{r}, t) = \frac{i}{\hbar} \int_{-\infty}^t dt' d_l(t') [E(\mathbf{r}, t), E_l(\mathbf{r}', t')] \quad (\text{A10})$$

is the electric field at (\mathbf{r}, t) generated by the dipole $\mathbf{d}(t')$ at \mathbf{r}' , whose explicit expression is given by Equation (39).

Some comments are in order. (i) While Equation (A2) is approximate, Equation (A10) is exact, as a consequence of the linearity of Maxwell's equations. (ii) E_{dip} is an operator containing both a molecule operator $\mathbf{d}(t)$ and an identity operator in Fock field space, as the field commutator is a c -number. This last property is also a consequence of the linearity of Maxwell's equations. (iii) This same procedure can be adapted to other sources. For instance, substituting $d_n(t') [E(\mathbf{r}, t), E_n(\mathbf{r}', t')]$ into Equation (A10) with (a) $m_n(t') [E(\mathbf{r}, t), B_n(\mathbf{r}', t')]$ generates the electric field at (\mathbf{r}, t) produced by a magnetic dipole $\mathbf{m}(t')$ at \mathbf{r}' , (b) $d_n(t') [B(\mathbf{r}, t), E_n(\mathbf{r}', t')]$ generates the magnetic field at (\mathbf{r}, t) caused by a electric dipole $\mathbf{d}(t')$ at $\mathbf{r} = \mathbf{r}'$, (c) $Q_{ln}(t') [E(\mathbf{r}, t), \partial'_l E_n(\mathbf{r}', t')]$ generates the electric field at (\mathbf{r}, t) induced by the quadrupole tensor $Q_{ln}(t')$ at position \mathbf{r}' , and so on. (iv) We could have reached these same conclusions from an approach analogous to our approach for

molecular susceptibility. Indeed, let us assume that the interaction Hamiltonian $H_{\text{Int}}(t')$ in the interaction picture is linear in the electric and magnetic fields. Now, we are not restricted to point sources. For example, it can be the field generated by prescribed classical charge and current fluctuations in a macroscopic body. Analogously to Equation (A1), we have

$$E(t) \approx E_0(t) - \frac{i}{\hbar} \int_{-\infty}^t dt' [E_0(t'), H_{\text{Int}}(t')]. \quad (\text{A11})$$

The second term in Equation (A11) can be recognized as the field produced by the source present in H_{Int} . For the electric dipole case, $H_{\text{Int}}(t) = -\mathbf{d}(t) \cdot \mathbf{E}(\mathbf{r}, t)$, and we immediately recover Equation (A10). However, notice that while Equation (A10) is exact, Equation (A11) is an approximation. Indeed, $[H_{\text{Int}}(t_1), [H_{\text{Int}}(t_2), E_0(t)]] \neq 0$, since the dipole operators in different instants of time do not commute. This reflects that, although Maxwell's equations are linear, the dipole induced in matter depends nonlinearly on the field, which, in turn, produces a nonlinearity in the time evolution of the electric field. Still, if H_{Int} depends only on material classical and prescribed variables, as in the aforementioned example of a macroscopic body, then Equation (A11) becomes an exact equation.

Appendix B. London Interaction in the Imaginary Frequency Domain

Here, we demonstrate the equivalence between Equation (64) and the expression that is usually employed in the literature [2]

$$E_{\text{London}} = -\frac{3\hbar}{32\pi^3\epsilon_0^2 r^6} \int_{-\infty}^{\infty} d\omega \alpha^A(i\omega) \alpha^B(i\omega). \quad (\text{A12})$$

From the fluctuation–dissipation theorem at zero temperature, we have

$$\eta^\zeta(\omega) = 2 \text{sgn}(\omega) \text{Im}[\alpha^\zeta(\omega)], \quad (\text{A13})$$

where the sign function is defined as $\text{sgn}(\omega) = \omega/|\omega|$. Substituting Equation (A13) into (64),

$$E_{\text{London}} = -\frac{3\hbar}{32\pi^3\epsilon_0^2 r^6} \int_{-\infty}^{\infty} d\omega \left(\text{Re}[\alpha^A(\omega)] \text{sgn}(\omega) \text{Im}[\alpha^B(\omega)] + \text{sgn}(\omega) \text{Im}[\alpha^A(\omega)] \text{Re}[\alpha^B(\omega)] \right). \quad (\text{A14})$$

Recalling that $\text{Re}[\alpha(\omega)]$ ($\text{Im}[\alpha(\omega)]$) is an even (odd) function, since $\alpha(\tau)$ is a real number, we obtain

$$E_{\text{London}} = -\frac{3\hbar}{16\pi^3\epsilon_0^2 r^6} \text{Im} \int_0^{\infty} d\omega \alpha^A(\omega) \alpha^B(\omega). \quad (\text{A15})$$

Causality implies that the polarizabilities are analytical in the superior half-plane [127], allowing us to perform a Wick rotation, leading to Equation (A12).

References

1. Dirac, P.A.M. The Quantum Theory of the Emission and Absorption of Radiation. *Proc. Royal Soc. Lond. A* **1927**, *114*, 243.
2. Craig, D.P.; Thirunamachandran, T. *Molecular Quantum Electrodynamics*; Dover Publications: New York, NY, USA, 1984.
3. Compagno, G.; Passante, R.; Persico, F. *Atom-Field Interactions and Dressed Atoms*; Cambridge University Press: Cambridge, UK, 1995.
4. Buhmann, S.Y. *Dispersion Forces I: Macroscopic Quantum Electrodynamics and Ground-State Casimir, Casimir–Polder and van der Waals Forces*; Springer: Cham, Switzerland, 2012.
5. Buhmann, S.Y. *Dispersion Forces II: Many-Body Effects, Excited Atoms, Finite Temperature and Quantum Friction*; Springer: Cham, Switzerland, 2012.
6. Milonni, P.W. *An Introduction to Quantum Optics and Quantum Fluctuations*; Oxford University Press: Oxford, UK, 2019.
7. Passante, R.; Power, E.A.; Thirunamachandran, T. Radiation-molecule coupling using dynamic polarizabilities: Application to many-body forces. *Phys. Lett. A* **1998**, *249*, 77. [[CrossRef](#)]
8. Passante, R.; Rizzuto, L. Effective Hamiltonians in nonrelativistic quantum electrodynamics. *Symmetry* **2021**, *13*, 2375. [[CrossRef](#)]
9. Alonso, L.; Matos, G.C.; Impens, F.; Neto, P.A.M.; de Melo e Souza, R. Multipole Approach to the Dynamical Casimir Effect with Finite-Size Scatterers. *Entropy* **2024**, *26*, 251. [[CrossRef](#)]

10. de Melo e Souza, R.; Impens, F.; Neto, P.A.M. Microscopic dynamical Casimir effect. *Phys. Rev. A* **2018**, *97*, 032514. [[CrossRef](#)]
11. Lo, L.; Law, C.K. Quantum radiation from a shaken two-level atom in vacuum. *Phys. Rev. A* **2018**, *98*, 063807. [[CrossRef](#)]
12. Belén Fariás, M.; Fosco, C.D.; Lombardo, F.C.; Mazzitelli, F.D. Motion induced radiation and quantum friction for a moving atom. *Phys. Rev. D* **2019**, *100*, 036013. [[CrossRef](#)]
13. Fosco, C.D.; Lombardo, F.C.; Mazzitelli, F.D. Motion-induced radiation due to an atom in the presence of a graphene plane. *Universe* **2021**, *7*, 158. [[CrossRef](#)]
14. Dalvit, D.A.R.; Kort-Kamp, W.J.M. Shaping dynamical Casimir photons. *Universe* **2021**, *7*, 189. [[CrossRef](#)]
15. Cohen-Tannoudji, C.; Dupont-Roc, J.; Grynberg, G. *Photons and Atoms: Introduction to Quantum Electrodynamics*; Wiley: New York, NY, USA, 1997.
16. Cresser, J.D. Electric field commutation relation in the presence of a dipole atom. *Phys. Rev. A* **1984**, *29*, 1984. [[CrossRef](#)]
17. Cresser, J.D. Unequal Time EM Field Commutators in Quantum Optics. *Phys. Scr.* **1988**, *T21*, 52. [[CrossRef](#)]
18. Milonni, P.W. *The Quantum Vacuum: An Introduction to Quantum Electrodynamics*; Academic Press: New York, NY, USA, 1994.
19. Brune, M.; Raimond, J.M.; Goy, P.; Davidovich, L.; Haroche, S. Realization of a two-photon maser oscillator. *Phys. Rev. Lett.* **1987**, *59*, 1899. [[CrossRef](#)]
20. Davidovich, L.; Raimond, J.M.; Brune, M.; Haroche, S. Quantum theory of a two-photon micromaser. *Phys. Rev. A* **1987**, *36*, 3771. [[CrossRef](#)]
21. Neto, P.A.M.; Davidovich, L.; Raimond, J.-M. Theory of the nondegenerate two-photon micromaser. *Phys. Rev. A* **1991**, *43*, 5073. [[CrossRef](#)]
22. Hayat, A.; Ginzburg, P.; Orenstein, M. Observation of two-photon emission from semiconductors. *Nat. Photonics* **2008**, *2*, 238. [[CrossRef](#)]
23. Wang, H.; Hu, H.; Chung, T.H.; Qin, J.; Yang, X.; Li, J.P.; Liu, R.Z.; Zhong, H.S.; He, Y.M.; Ding, X.; et al. On-demand semiconductor source of entangled photons which simultaneously has high fidelity, efficiency, and indistinguishability. *Phys. Rev. Lett.* **2019**, *122*, 113602. [[CrossRef](#)]
24. Zhang, J.; Ma, J.; Parry, M.; Cai, M.; Camacho-Morales, R.; Xu, L.; Neshev, D.N.; Sukhorukov, A.A. Spatially entangled photon pairs from lithium niobate nonlocal metasurfaces. *Sci. Adv.* **2022**, *8*, eabq4240. [[CrossRef](#)]
25. Poddubny, A.N.; Ginzburg, P.; Belov, P.A.; Zayats, A.V.; Kivshar, Y.S. Tailoring and enhancing spontaneous two-photon emission using resonant plasmonic nanostructures. *Phys. Rev. A* **2012**, *86*, 033826. [[CrossRef](#)]
26. Muniz, Y.; Manjavacas, A.; Farina, C.; Dalvit, D.A.R.; Kort-Kamp, W.J.M. Two-photon spontaneous emission in atomically thin plasmonic nanostructures. *Phys. Rev. Lett.* **2020**, *125*, 033601. [[CrossRef](#)]
27. Hu, F.; Li, L.; Liu, Y.; Meng, Y.; Gong, M.; Yang, Y. Two-plasmon spontaneous emission from a nonlocal epsilon-near-zero material. *Commun. Phys.* **2021**, *4*, 84. [[CrossRef](#)]
28. Muniz, Y.; Abrantes, P.P.; Martín-Moreno, L.; Pinheiro, F.A.; Farina, C.; Kort-Kamp, W.J.M. Entangled two-plasmon generation in carbon nanotubes and graphene-coated wires. *Phys. Rev. B* **2022**, *105*, 165412. [[CrossRef](#)]
29. Smeets, S.; Maes, B.; Rosolen, G. General framework for two-photon spontaneous emission near plasmonic nanostructures. *Phys. Rev. A* **2023**, *107*, 063516. [[CrossRef](#)]
30. Feinberg, G.; Sucher, J. General Theory of the van der Waals Interaction: A model-independent approach. *Phys. Rev. A* **1970**, *2*, 2395. [[CrossRef](#)]
31. Farina, C.; Santos, F.C.; Tort, A.C. On the force between an electrically polarizable atom and a magnetically polarizable one. *J. Phys. A* **2002**, *35*, 2477. [[CrossRef](#)]
32. Förster, T. Energiewanderung und fluoreszenz. *Naturwissenschaften* **1946**, *33*, 166. [[CrossRef](#)]
33. Martínez, P.L.H.; Govorov, A.; Demir, H.V. *Understanding and Modeling Förster-Type Resonance Energy Transfer (FRET)*; Springer: Singapore, 2017; Volume 1.
34. Milonni, P.W.; Rafsanjani, S.M.H. Distance dependence of two-atom dipole interactions with one atom in an excited state. *Phys. Rev. A* **2015**, *92*, 062711. [[CrossRef](#)]
35. Biehs, S.-A.; Menon, V.M.; Agarwal, G.S. Long-range dipole-dipole interaction and anomalous Förster energy transfer across a hyperbolic metamaterial. *Phys. Rev. B* **2016**, *93*, 245439. [[CrossRef](#)]
36. Weeraddana, D.; Premaratne, M.; Gunapala, S.D.; Andrews, D.L. Controlling resonance energy transfer in nanostructure emitters by positioning near a mirror. *J. Chem. Phys.* **2017**, *147*, 074117. [[CrossRef](#)]
37. Li, Y.; Nemilentsau, A.; Argyropoulos, C. Resonance energy transfer and quantum entanglement mediated by epsilon-near-zero and other plasmonic waveguide systems. *Nanoscale* **2019**, *11*, 14635. [[CrossRef](#)]
38. Abrantes, P.P.; Szilard, D.; Rosa, F.S.S.; Farina, C. Resonance energy transfer at percolation transition. *Mod. Phys. Lett. A* **2020**, *35*, 2040022. [[CrossRef](#)]
39. Abrantes, P.P.; Bastos, G.; Szilard, D.; Farina, C.; Rosa, F.S.S. Tuning resonance energy transfer with magneto-optical properties of graphene. *Phys. Rev. B* **2021**, *103*, 174421. [[CrossRef](#)]
40. Pini, F.; Francés-Soriano, L.; Andriago, V.; Natile, M.M.; Hildebrandt, N. Optimizing upconversion nanoparticles for FRET biosensing. *ACS Nano* **2023**, *17*, 4971. [[CrossRef](#)]
41. Nayem, S.H.; Sikder, B.; Uddin, S.Z. Anisotropic energy transfer near multi-layer black phosphorus. *2D Mater.* **2023**, *10*, 045022. [[CrossRef](#)]

42. Song, Q.; Yan, X.; Cui, H.; Ma, M. Efficient cascade resonance energy transfer in dynamic nanoassembly for intensive and long-lasting multicolor chemiluminescence. *ACS Nano* **2020**, *14*, 3696. [\[CrossRef\]](#)
43. Rusanen, J.; Kareinen, L.; Levanov, L.; Mero, S.; Pakkanen, S.H.; Kantele, A.; Amanat, F.; Krammer, F.; Hedman, K.; Vapalahti, O.; et al. A 10-Minute “Mix and Read” Antibody Assay for SARS-CoV-2. *Viruses* **2021**, *13*, 143. [\[CrossRef\]](#)
44. Bednarz, A.; Sønderskov, S.M.; Dong, M.; Birkedal, V. Ion-mediated control of structural integrity and reconfigurability of DNA nanostructures. *Nanoscale* **2023**, *15*, 1317. [\[CrossRef\]](#)
45. Andrews, D.L.; Sherborne, B.S. Resonant excitation transfer: A quantum electrodynamical study. *J. Chem. Phys.* **1987**, *86*, 4011. [\[CrossRef\]](#)
46. Franz, J.C.; Buhmann, S.Y.; Salam, A. Macroscopic quantum electrodynamics theory of resonance energy transfer involving chiral molecules. *Phys. Rev. A* **2023**, *107*, 032809. [\[CrossRef\]](#)
47. Craig, D.P.; Power, E.A. The asymptotic Casimir–Polder potential from second-order perturbation theory and its generalization for anisotropic polarizabilities. *Int. J. Quantum Chem.* **1969**, *3*, 903. [\[CrossRef\]](#)
48. Cohen-Tannoudji, C.; Diu, B.; Laloë, F. *Quantum Mechanics*; Wiley-VCH: Weinheim, Germany, 2019; Volume II.
49. London, F. Zur Theorie und Systematik der Molekularkräfte. *Z. Phys.* **1930**, *63*, 245. [\[CrossRef\]](#)
50. Casimir, H.B.G.; Polder, D. The influence of retardation on the London-van der Waals forces. *Phys. Rev.* **1948**, *73*, 360. [\[CrossRef\]](#)
51. Power, E.A.; Thirunamachandran, T. Dispersion forces between molecules with one or both molecules excited. *Phys. Rev. A* **1995**, *51*, 3660. [\[CrossRef\]](#)
52. Power, E.A.; Thirunamachandran, T. Two- and three-body dispersion forces with one excited molecule. *Chem. Phys.* **1995**, *198*, 5. [\[CrossRef\]](#)
53. Rizzuto, L.; Passante, R.; Persico, F. Dynamical Casimir-Polder energy between an excited- and a ground-state atom. *Phys. Rev. A* **2004**, *70*, 012107. [\[CrossRef\]](#)
54. Barcellona, P.; Passante, R.; Rizzuto, L.; Buhmann, S.Y. van der Waals interactions between excited atoms in generic environments. *Phys. Rev. A* **2016**, *94*, 012705. [\[CrossRef\]](#)
55. Kien, F.L.; Kornovan, D.F.; Chormaic, S.N.; Busch, T. Repulsive Casimir-Polder potentials of low-lying excited states of a multilevel alkali-metal atom near an optical nanofiber. *Phys. Rev. A* **2022**, *105*, 042817. [\[CrossRef\]](#)
56. Lu, B.-S.; Arifa, K.Z.; Ducloy, M. An excited atom interacting with a Chern insulator: Toward a far-field resonant Casimir–Polder repulsion. *Eur. Phys. J. D* **2022**, *76*, 210. [\[CrossRef\]](#)
57. Jenkins, J.K.; Salam, A.; Thirunamachandran, T. Retarded dispersion interaction energies between chiral molecules. *Phys. Rev. A* **1994**, *50*, 4767. [\[CrossRef\]](#)
58. Salam, A. On the effect of a radiation field in modifying the intermolecular interaction between two chiral molecules. *J. Chem. Phys.* **2006**, *124*, 014302. [\[CrossRef\]](#)
59. Butcher, D.T.; Buhmann, S.Y.; Scheel, S. Casimir-Polder forces between chiral objects. *New J. Phys.* **2012**, *14*, 11301. [\[CrossRef\]](#)
60. Barcellona, P.; Safari, H.; Salam, A.; Buhmann, S.Y. Enhanced chiral discriminatory van der Waals interactions mediated by chiral surfaces. *Phys. Rev. Lett.* **2017**, *118*, 193401. [\[CrossRef\]](#)
61. Wylie, J.M.; Sipe, J.E. Quantum electrodynamics near an interface. II. *Phys. Rev. A* **1985**, *32*, 2030. [\[CrossRef\]](#)
62. Buhmann, S.Y.; Welsch, D.-G.; Kampf, T. Ground-state van der Waals forces in planar multilayer magnetodielectrics. *Phys. Rev. A* **2005**, *72*, 032112. [\[CrossRef\]](#)
63. Dalvit, D.A.R.; Neto, P.A.M.; Lambrecht, A.; Reynaud, S. Probing quantum-vacuum geometrical effects with cold atoms. *Phys. Rev. Lett.* **2008**, *100*, 040405. [\[CrossRef\]](#)
64. Messina, R.; Dalvit, D.A.R.; Neto, P.A.M.; Lambrecht, A.; Reynaud, S. Dispersive interactions between atoms and nonplanar surfaces. *Phys. Rev. A* **2009**, *80*, 022119. [\[CrossRef\]](#)
65. Contreras-Reyes, A.M.; Guérout, R.; Neto, P.A.M.; Dalvit, D.A.R.; Lambrecht, A.; Reynaud, S. Casimir-Polder interaction between an atom and a dielectric grating. *Phys. Rev. A* **2010**, *82*, 052517. [\[CrossRef\]](#)
66. Cysne, T.; Kort-Kamp, W.J.M.; Oliver, D.; Pinheiro, F.A.; Rosa, F.S.S.; Farina, C. Tuning the Casimir-Polder interaction via magneto-optical effects in graphene. *Phys. Rev. A* **2014**, *90*, 052511. [\[CrossRef\]](#)
67. Bimonte, G.; Emig, T.; Kardar, M. Casimir-Polder interaction for gently curved surfaces. *Phys. Rev. D* **2014**, *90*, 081702(R). [\[CrossRef\]](#)
68. Bimonte, G.; Emig, T.; Kardar, M. Casimir-Polder force between anisotropic nanoparticles and gently curved surfaces. *Phys. Rev. D* **2015**, *92*, 025028. [\[CrossRef\]](#)
69. Garcion, C.; Fabre, N.; Bricha, H.; Perales, F.; Scheel, S.; Ducloy, M.; Dutier, G. Intermediate-range Casimir-Polder interaction probed by high-order slow atom diffraction. *Phys. Rev. Lett.* **2021**, *127*, 170402. [\[CrossRef\]](#)
70. Abrantes, P.P.; Pessanha, V.; de Melo e Souza, R.; Farina, C. Controlling the atom-sphere interaction with an external electric field. *Phys. Rev. A* **2021**, *104*, 022820. [\[CrossRef\]](#)
71. Marachevsky, V.N.; Sidelnikov, A.A. Casimir-Polder interaction with Chern-Simons boundary layers. *Phys. Rev. D* **2023**, *107*, 105019. [\[CrossRef\]](#)
72. Alves, D.T.; Queiroz, L.; Nogueira, E.C.M.; Peres, N.M.R. Curvature-induced repulsive effect on the lateral Casimir-Polder–van der Waals force. *Phys. Rev. A* **2023**, *107*, 062821. [\[CrossRef\]](#)
73. Fosco, C.D.; Lombardo, F.C.; Mazzitelli, F.D. Casimir physics beyond the proximity force approximation: The derivative expansion. *Physics* **2024**, *6*, 290. [\[CrossRef\]](#)

74. Messina, R.; Vasile, R.; Passante, R. Dynamical Casimir-Polder force on a partially dressed atom near a conducting wall. *Phys. Rev. A* **2010**, *82*, 062501. [\[CrossRef\]](#)
75. Behunin, R.O.; Hu, B.-L. Nonequilibrium forces between atoms and dielectrics mediated by a quantum field. *Phys. Rev. A* **2011**, *84*, 012902. [\[CrossRef\]](#)
76. Barcellona, P.; Passante, R.; Rizzuto, L.; Buhmann, S.Y. Dynamical Casimir-Polder interaction between a chiral molecule and a surface. *Phys. Rev. A* **2016**, *93*, 032508. [\[CrossRef\]](#)
77. Goedecke, G.H.; Wood, R.C. Casimir-Polder interaction at finite temperature. *Phys. Rev. A* **1999**, *11*, 2577. [\[CrossRef\]](#)
78. Barton, G. Long-range Casimir-Polder-Feinberg-Sucher intermolecular potential at nonzero temperature. *Phys. Rev. A* **2001**, *64*, 032102. [\[CrossRef\]](#)
79. Obrecht, J.M.; Wild, R.J.; Antezza, M.; Pitaevskii, L.P.; Stringari, S.; Cornell, E.A. Measurement of the Temperature Dependence of the Casimir-Polder Force. *Phys. Rev. Lett.* **2007**, *98*, 063201. [\[CrossRef\]](#)
80. Haakh, H.; Intravaia, F.; Henkel, C.; Spagnolo, S.; Passante, R.; Power, B.; Sols, F. Temperature dependence of the magnetic Casimir-Polder interaction. *Phys. Rev. A* **2009**, *80*, 062905. [\[CrossRef\]](#)
81. Chaichian, M.; Klimchitskaya, G.L.; Mostepanenko, V.M.; Tureanu, A. Thermal Casimir-Polder interaction of different atoms with graphene. *Phys. Rev. A* **2012**, *86*, 012515. [\[CrossRef\]](#)
82. Laliotis, A.; de Silans, T.P.; Maurin, I.; Ducloy, M.; Bloch, D. Casimir-Polder interactions in the presence of thermally excited surface modes. *Nat. Commun.* **2014**, *5*, 4364. [\[CrossRef\]](#)
83. Khusnutdinov, N.; Kashapov, R.; Woods, L.M. Thermal Casimir and Casimir-Polder interactions in N parallel 2D Dirac materials. *2D Mater.* **2018**, *5*, 035032. [\[CrossRef\]](#)
84. Israelachvili, J.N. *Intermolecular and Surface Forces*; Academic Press: Waltham, MA, USA, 2011.
85. Geim, A.K.; Grigorieva, I.V. Van der Waals heterostructures. *Nature* **2013**, *499*, 419. [\[CrossRef\]](#)
86. Liu, Y.; Weiss, N.O.; Duan, X.; Cheng, H.-C.; Huang, Y.; Duan, X. Van der Waals heterostructures and devices. *Nat. Rev. Mater.* **2016**, *1*, 16042. [\[CrossRef\]](#)
87. Castellanos-Gomez, A.; Duan, X.; Fei, Z.; Gutierrez, H.R.; Huang, Y.; Huang, X.; Quereda, J.; Qian, Q.; Sutter, E.; Sutter, P. Van der Waals heterostructures. *Nat. Rev. Methods Primers* **2022**, *2*, 58. [\[CrossRef\]](#)
88. Caldeweyher, E.; Ehlert, S.; Hansen, A.; Neugebauer, H.; Spicher, S.; Bannwarth, C.; Grimme, S. A generally applicable atomic-charge dependent London dispersion correction. *J. Chem. Phys.* **2019**, *150*, 154122. [\[CrossRef\]](#)
89. Caldeweyher, E.; Mewes, J.-M.; Ehlert, S.; Grimme, S. Extension and evaluation of the D4 London-dispersion model for periodic systems. *Phys. Chem. Chem. Phys.* **2020**, *22*, 8499. [\[CrossRef\]](#)
90. Chowdhury, S.T.u.R.; Tang, H.; Perdew, J.P. van der Waals corrected density functionals for cylindrical surfaces: Ammonia and nitrogen dioxide adsorbed on a single-walled carbon nanotube. *Phys. Rev. B* **2021**, *103*, 195410. [\[CrossRef\]](#)
91. Dryden, D.M.; Hopkins, J.C.; Denoyer, L.K.; Poudel, L.; Steinmetz, N.F.; Ching, W.-Y.; Podgornik, R.; Parsegian, A.; French, R.H. van der Waals Interactions on the Mesoscale: Open-Science Implementation, Anisotropy, Retardation, and Solvent Effects. *Langmuir* **2015**, *31*, 10145. [\[CrossRef\]](#)
92. Spreng, B.; Neto, P.A.M.; Ingold, G.-L. Plane-wave approach to the exact van der Waals interaction between colloid particles. *J. Chem. Phys.* **2020**, *153*, 024115. [\[CrossRef\]](#)
93. Nunes, R.O.; Spreng, B.; de Melo e Souza, R.; Ingold, G.-L.; Neto, P.A.M.; Rosa, F.S.S. The Casimir Interaction between Spheres Immersed in Electrolytes. *Universe* **2021**, *7*, 156. [\[CrossRef\]](#)
94. Scheel, S.; Buhmann, S.Y. Casimir-Polder forces on moving atoms. *Phys. Rev. A* **2009**, *80*, 042902. [\[CrossRef\]](#)
95. Barton, G. On van der Waals friction: I. Between two atoms. *New J. Phys.* **2010**, *12*, 113044. [\[CrossRef\]](#)
96. Pieplow, G.; Henkel, C. Fully covariant radiation force on a polarizable particle. *New J. Phys.* **2013**, *15*, 023027. [\[CrossRef\]](#)
97. Intravaia, F.; Behunin, R.O.; Dalvit, D.A.R. Quantum friction and fluctuation theorems. *Phys. Rev. A* **2014**, *89*, 050101(R). [\[CrossRef\]](#)
98. Intravaia, F.; Behunin, R.O.; Henkel, C.; Busch, K.; Dalvit, D.A.R. Failure of Local Thermal Equilibrium in Quantum Friction. *Phys. Rev. Lett.* **2016**, *117*, 100402. [\[CrossRef\]](#)
99. Donaire, M.; Lambrecht, A. Velocity-dependent dipole forces on an excited atom. *Phys. Rev. A* **2016**, *93*, 022701. [\[CrossRef\]](#)
100. Reiche, D.; Intravaia, F.; Hsiang, J.-T.; Busch, K.; Hu, B.L. Nonequilibrium thermodynamics of quantum friction. *Phys. Rev. A* **2020**, *102*, 050203(R). [\[CrossRef\]](#)
101. Reiche, D.; Busch, K.; Intravaia, F. Nonadditive Enhancement of Nonequilibrium Atom-Surface Interactions. *Phys. Rev. Lett.* **2020**, *124*, 193603. [\[CrossRef\]](#)
102. Fariás, M.B.; Lombardo, F.C.; Soba, A.; Villar, P.I.; Decca, R.S. Towards detecting traces of non-contact quantum friction in the corrections of the accumulated geometric phase. *NPJ Quantum Inf.* **2020**, *6*, 25. [\[CrossRef\]](#)
103. Lombardo, F.C.; Decca, R.S.; Viotti, L.; Villar, P.I. Detectable Signature of Quantum Friction on a Sliding Particle in Vacuum. *Adv. Quantum Technol.* **2021**, *4*, 2000155. [\[CrossRef\]](#)
104. Dedkov, G.V.; Kyasov, A.A. Nonlocal friction forces in the particle-plate and plate-plate configurations: Nonretarded approximation. *Surf. Sci.* **2020**, *700*, 121681. [\[CrossRef\]](#)
105. Dedkov, G.V. Van der Waals Interactions of Moving Particles with Surfaces of Cylindrical Geometry. *Universe* **2021**, *7*, 106. [\[CrossRef\]](#)
106. Impens, F.; Behunin, R.O.; Ttira, C.C.; Neto, P.A.M. Non-local double-path Casimir phase in atom interferometers. *EPL* **2013**, *101*, 60006. [\[CrossRef\]](#)

107. Impens, F.; Ttira, C.C.; Neto, P.A.M. Non-additive dynamical Casimir atomic phases. *J. Phys. B At. Mol. Opt. Phys.* **2013**, *46*, 245503. [\[CrossRef\]](#)
108. Impens, F.; de Melo e Souza, R.; Matos, G.C.; Neto, P.A.M. Dynamical Casimir effects with atoms: From the emission of photon pairs to geometric phases. *EPL* **2022**, *138*, 30001. [\[CrossRef\]](#)
109. Salam, A. van der Waals Dispersion Potential between Excited Chiral Molecules via the Coupling of Induced Dipoles. *Physics* **2023**, *5*, 247. [\[CrossRef\]](#)
110. Dung, H.T. Interatomic dispersion potential in a cylindrical system: Atoms being off axis. *J. Phys. B* **2016**, *49*, 165502. [\[CrossRef\]](#)
111. Zuki, F.M.; Edyvean, R.G.J.; Pourzolfaghar, H.; Kasim, N. Modeling of the Van Der Waals Forces during the Adhesion of Capsule-Shaped Bacteria to Flat Surfaces. *Biomimetics* **2021**, *6*, 5. [\[CrossRef\]](#)
112. Laliotis, A.; Lu, B.-S.; Ducloy, M.; Wilkowski, D. Atom-surface physics: A review. *AVS Quantum Sci.* **2021**, *3*, 043501. [\[CrossRef\]](#)
113. Nogueira, E.C.M.; Queiroz, L.; Alves, D.T. Peak, valley, and intermediate regimes in the lateral van der Waals force. *Phys. Rev. A* **2021**, *104*, 012816. [\[CrossRef\]](#)
114. Nogueira, E.C.M.; Queiroz, L.; Alves, D.T. Sign inversion in the lateral van der Waals force. *Phys. Rev. A* **2022**, *105*, 062816. [\[CrossRef\]](#)
115. Milonni, P.W.; Ackerhalt, J.R.; Smith, W.A. Interpretation of Radiative Corrections in Spontaneous Emission. *Phys. Rev. Lett.* **1973**, *31*, 958. [\[CrossRef\]](#)
116. Dalibard, J.; Dupont-Roc, J.; Cohen-Tannoudji, C. Vacuum fluctuations and radiation reaction: Identification of their respective contributions. *J. Phys.* **1982**, *43*, 1617. [\[CrossRef\]](#)
117. Cohen-Tannoudji, C. Fluctuations in Radiative Processes. *Phys. Scr.* **1986**, *12*, 19. [\[CrossRef\]](#)
118. Zhou, W.; Cheng, S.; Yu, H. Interatomic interaction of two ground-state atoms in vacuum: Contributions of vacuum fluctuations and radiation reaction. *Phys. Rev. A* **2021**, *103*, 012227. [\[CrossRef\]](#)
119. Impens, F.; Ttira, C.C.; Behunin, R.O.; Neto, P.A.M. Dynamical local and nonlocal Casimir atomic phases. *Phys. Rev. A* **2014**, *89*, 022516. [\[CrossRef\]](#)
120. Matos, C.G.; de Melo e Souza, R.; Neto, P.A.M.; Impens, F. Quantum Vacuum Sagnac Effect. *Phys. Rev. Lett.* **2021**, *127*, 270401.
121. Breuer, H.P.; Petruccione, F. *The Theory of Open Quantum Systems*; Oxford University Press: Oxford, UK, 2002.
122. Calzetta, E.A.; Hu, B.-L.B. *Nonequilibrium Quantum Field Theory*; Cambridge University Press: Cambridge, UK, 2022.
123. Weiss, U. *Quantum Dissipative Systems*; World Scientific: Singapore, 2007.
124. Kubo, R. The fluctuation-dissipation theorem. *Rep. Prog. Phys.* **1966**, *29*, 255. [\[CrossRef\]](#)
125. Dubovik, V.M.; Tugushev, V.V. Toroid moments in electrodynamics and solid-state physics. *Phys. Rep.* **1990**, *187*, 142. [\[CrossRef\]](#)
126. Pitombo, R.S.; Vasconcellos, M.; Farina, C.; de Melo e Souza, R. Source method for the evaluation of multipole fields. *Eur. J. Phys.* **2021**, *42*, 025202. [\[CrossRef\]](#)
127. Nussenzveig, H.M. *Causality and Dispersion Relations*; Academic Press: New York, NY, USA, 1972.

Disclaimer/Publisher's Note: The statements, opinions and data contained in all publications are solely those of the individual author(s) and contributor(s) and not of MDPI and/or the editor(s). MDPI and/or the editor(s) disclaim responsibility for any injury to people or property resulting from any ideas, methods, instructions or products referred to in the content.